Technical Note

TN no. N-1561
(FAA-RD-79-11)

title: SHRINKAGE-COMPENSATING CEMENT FOR AIRPORT PAVEMENT: Phase 2

author: John R. Keeton

date: November 1979

sponsor: U. S. Department of Transportation
Federal Aviation Administration

program nos: 52-040

CIVIL ENGINEERING LABORATORY
NAVAL CONSTRUCTION BATTALION CENTER
Port Hueneme, California 93043

Unclassified

SECURITY CLASSIFICATION OF THIS PAGE *(When Data Entered)*

REPORT DOCUMENTATION PAGE		READ INSTRUCTIONS BEFORE COMPLETING FORM
1. REPORT NUMBER TN-1561	2. GOVT ACCESSION NO. DN587103	3. RECIPIENT'S CATALOG NUMBER
4. TITLE *(and Subtitle)* SHRINKAGE-COMPENSATING CEMENT FOR AIRPORT PAVEMENT: Phase 2		5. TYPE OF REPORT & PERIOD COVERED Final; Jan 75 – Jan 79 6. PERFORMING ORG. REPORT NUMBER
7. AUTHOR(s) John R. Keeton		8. CONTRACT OR GRANT NUMBER(s)
9. PERFORMING ORGANIZATION NAME AND ADDRESS CIVIL ENGINEERING LABORATORY Naval Construction Battalion Center Port Hueneme, California 93043		10. PROGRAM ELEMENT, PROJECT, TASK AREA & WORK UNIT NUMBERS 52-040
11. CONTROLLING OFFICE NAME AND ADDRESS U.S. Department of Transportation, Federal Aviation Administration, Systems Research & Development Service Washington, D. C. 20590		12. REPORT DATE November 1979 13. NUMBER OF PAGES 45
14. MONITORING AGENCY NAME & ADDRESS*(if different from Controlling Office)*		15. SECURITY CLASS. *(of this report)* Unclassified 15a. DECLASSIFICATION/DOWNGRADING SCHEDULE

16. DISTRIBUTION STATEMENT *(of this Report)*

Approved for public release; distribution unlimited.

17. DISTRIBUTION STATEMENT *(of the abstract entered in Block 20, if different from Report)*

18. SUPPLEMENTARY NOTES

19. KEY WORDS *(Continue on reverse side if necessary and identify by block number)*

Shrinkage-compensating concrete, airport pavement.

20. ABSTRACT *(Continue on reverse side if necessary and identify by block number)*

Details of a research study on shrinkage-compensating concrete for airport pavements are presented. A total of 53 slab-type prisms 1 foot square and 8, 12, 16, or 20 inches thick were subjected to shrinkage, cooling, and heating. Concrete compressive stresses induced by expansion were calculated, as well as residual compressive stresses after losses due to shrinkage and cooling. The residual concrete compressive stresses, coupled with

continued

DD FORM 1 JAN 73 1473 EDITION OF 1 NOV 65 IS OBSOLETE

Unclassified

SECURITY CLASSIFICATION OF THIS PAGE *(When Data Entered)*

20. Continued

results from previous field applications of shrinkage-compensating concrete, are used as a basis for recommendation of transverse joint spacings up to 200 feet.

Library Card

Civil Engineering Laboratory
SHRINKAGE-COMPENSATING CEMENT FOR AIRPORT PAVEMENT: Phase 2 (Final), by John R. Keeton
TN-1561 45 pp illus November 1979 Unclassified

1. Shrinkage-compensating concrete 2. Airport pavement I. 52-040

Details of a research study on shrinkage-compensating concrete for airport pavements are presented. A total of 53 slab-type prisms 1 foot square and 8, 12, 16, or 20 inches thick were subjected to shrinkage, cooling, and heating. Concrete compressive stresses induced by expansion were calculated, as well as residual compressive stresses after losses due to shrinkage and cooling. The residual concrete compressive stresses, coupled with results from previous field applications of shrinkage-compensating concrete, are used as a basis for recommendation of transverse joint spacings up to 200 feet.

CONTENTS

INTRODUCTION

Historically, the determination of transverse joint spacing in portland cement concrete airport pavements has been dictated by consideration for shrinkage, temperature, warping and curling stresses, and subgrade friction. The present Federal Aviation Administration (FAA) practice of using transverse joint spacing of 25 feet has resulted from a combination of mathematical design calculations and observance of field performances of several joint spacings through the years. It is well known that concrete is weak in tension; therefore, either the concrete must be reinforced to hold cracks together or to provide flexural beam strength, or the "pieces" of concrete must be limited to size or length to preclude formation of severe cracks due to shrinkage or temperature changes (which cause curling or warping stresses).

The purpose of using expansive concrete in airport pavements is to induce sufficient compression into the concrete before it is placed in service to enable it to undergo the expected stresses without distress. This research was undertaken to provide quantitative values for residual concrete compressive stresses in lightly reinforced, thick, concrete slabs using shrinkage-compensating expansive concrete. These residual compressive stresses, in turn, are used to determine extended transverse joint spacings for slabs made with expansive concrete.

Successful utilization of any of the expansive cement concretes depends upon the amount and type of resistance to the expansion of the concrete. An expansive cement concrete in which no resistance is provided to the expansion shows greatly reduced mechanical properties. In the language of the expansive cement industry, the resistance to expansion is called "restraint." Restraint can be either external, as in the case of rigid framework, or internal, in the form of reinforcing steel or mesh. Some degree of restraint can also be provided by such forces as subgrade friction and by abutting structures. In the case of reinforcing steel or mesh, the developing bond strength provides the necessary restraint to expansion. Expansion of the concrete, resisted by the steel, places the steel in tension. This, in turn, places the concrete in compression, much as in prestressed concrete; generally speaking, the more the restraint (percent of reinforcement), the less the expansion and the more the induced compression in the concrete. Most field installations of shrinkage-compensating concretes have utilized successfully the amount, kind, and position of reinforcement required for the given structure.

Since little or no research had been done on expansive concretes in thick, lightly reinforced slabs, it was decided to limit the prismatic specimen thickness to 8, 12, 16, and 20 inches but to include many steel reinforcement percentages. Test results would then enable development

of a usable relationship between residual compressive stresses and steel percentage for pavement slabs up to 20 inches thick.

BACKGROUND

The FAA outlined an engineering and development need to determine the suitability and practicability of utilizing expansive cement concretes in construction of civil airport pavements. The benefits anticipated from the use of expansive cement concretes include reduced number of joints and increased strength and durability. The Engineering Requirement divided the program into two parts: Phase 1, Evaluation of Past and Current Investigation, to include plans for accomplishing needed research; and Phase 2, Laboratory Experiments and Analyses. The stated objectives include material specifications for expansive cement concretes and relationships between joint spacings and all factors influencing the spacing. The Civil Engineering Laboratory (CEL), Port Hueneme, Calif., contracted to accomplish the research. Results of the Phase 1 investigation were presented in Reference 1. Preliminary results and recommendations for future research on Phase 3, Shrinkage Compensating Cement in Fibrous Concrete, are presented in Appendix A.

EXPERIMENTAL PROGRAM - PHASE 2

The experimental program utilized to furnish research data to enable accomplishment of the objectives is summarized in Table 1 and outlined below.

Slab-type Prismatic Specimens

To provide basic research data which incorporate the unique thickness and mass of airport pavements, slab-type prismatic specimens were utilized as follows.

1. 12 by 12 inches in plan
   a. 8 inches thick
   b. 12 inches thick
   c. 16 inches thick
   d. 20 inches thick
2. 14 by 14 inches in plan
   a. 16 inches thick
   b. 20 inches thick

To simulate a full-size concrete slab exposed to the elements only at the top, all surfaces except the top were sealed with a butyl coating to prevent escape of moisture. Figure 1 shows some of the prisms in one of the drying environments.

---

1. Keeton, John R., "Shrinkage-Compensating Cement for Airport Pavement," Federal Aviation Administration Report No. FAA-RD-75-89, June 1975.

Instrumentation and Measurements

Both steel and concrete strain were measured with electrical resistance strain gages as soon as practicable after casting of the concrete. Steel strains were measured with weldable gages and concrete strain with embeddable strain gages. Strain gage readings were recorded initially on an automatic electronic data logger and, subsequently, on a portable strain indicator. Strain test data are reported in microstrain (i.e., μin./in.). On some of the figures, strain is also shown in percent.

Reinforcing Steel - Smooth, Welded Wire Fabric

Smooth, welded wire fabric in several typical sizes and grid spacings were used as reinforcing steel in the experimental prisms, as outlined in Table 1. One of the 6 by 6-inch welded wire fabric pieces instrumented with a weldable strain gage is shown in Figure 2. In accordance with FAA procedures (Ref 2), welded wire fabric was placed in each prism at a depth equal to one-fourth of the thickness plus 1 inch, measured from the top. For example, for a 16-inch-thick prism, the steel was placed at (¼ x 16) + 1 (i.e., 5 inches) from the top. Welded wire fabric sizes used in the study were the only ones available in small quantities.

Embeddable Strain Gages

Gages for measuring concrete strain were an embeddable type consisting of a single wire about 5 inches long, cast in plastic. One of the gages is shown in Figure 3. In all prisms, embedded strain gages were placed at one-fourth and three-fourths of the thickness, measured from the top. For example, for a prism 16 inches thick, embeddable gages were placed ¼ x 16 - or 4 - inches from the top and 3/4 x 16 - or 12 - inches from the top. Later in the study, some prisms also had embeddable gages 1 inch from the top and at mid-depth.

Curing

Following final set, the experimental prisms were cured under wet burlap for 24 hours, when the sides were sealed with a butyl rubber coating and a piece of wet burlap placed over the top surface. The wet burlap was then covered with aluminum foil for a total curing period of 28 days. Typical field-slab curing would probably be with a curing compound which would erode away gradually by exposure to the elements and to traffic. To enable the top surface of the concrete prisms to be free to emit moisture (shrink), it was decided not to use a curing compound in this study. The burlap, saturated with water when placed on the top of the prism, gradually dried over the next 27 days, simulating the action of a curing compound. At 28 days, the prisms were placed in a drying environment. Figure 4 shows some of the prisms during the curing period.

---

2. Federal Aviation Administration, Advisory Circular 150/5320-6B, Airport Pavement Design and Evaluation, May 28, 1974, pp. 73, 74.

Figure 1. Prismatic slab-type specimens in drying environment.

Figure 2. Typical 6 by 6-inch welded wire fabric instrumented with weldable strain gage.

TABLE 1. RESEARCH PROGRAM

Prism Size, in.		Aggregate Type[a]	Welded Wire Fabric		Steel Percentage[c]	Number of Prisms in Each Storage Humidity[d]
Plan	Thickness		Section, in.	Wire Size[b]		
12 x 12	8	L	6 x 6	No. 3 x No. 3	0.098L,T	1 - 50, 1 - 75
12 x 12	8	R	6 x 6	No. 3 x No. 3	0.098L,T	1 - 50, 1 - 75
12 x 12	12	L	None	None	0.0	1 - 50
12 x 12	12	L	6 x 6	No. 3 x No. 3	0.065L,T	1 - 50
				No. 2 x No. 2	0.075L,T	1 - 50, 1 - 75
				1/0 x 1/0	0.103L,T	1 - 50
				2/0 x 2/0	0.119L,T	1 - 50
				3/0 x 3/0	0.143L,T	2 - 50
				4/0 x 4/0	0.169L,T	1 - 50
12 x 12	12	R	6 x 6	No. 2 x No. 2	0.075L,T	1 - 50, 1 - 75
				1/0 x 1/0	0.103L,T	1 - 50, 1 - 75
				3/0 x 3/0	0.143L,T	1 - 50
12 x 12	16	L	None	None	0.0	1 - 50
12 x 12	16	L	6 x 6	No. 2 x No. 2	0.056L,T	1 - 50
				1/0 x 1/0	0.077L,T	1 - 50
				3/0 x 3/0	0.107L,T	2 - 50, 1 - 75
				5/0 x 5/0	0.152L,T	2 - 50, 2 - 75
12 x 12	16	R	6 x 6	1/0 x 1/0	0.077L,T	1 - 50, 1 - 75
				5/0 x 5/0	0.152L,T	1 - 50
12 x 12	20	L	None	None	0.0	1 - 50
12 x 12	20	L	6 x 6	2/0 x 2/0	0.072L,T	1 - 50
				4/0 x 4/0	0.102L,T	2 - 50, 1 - 75
				6/0 x 6/0	0.139L,T	2 - 50
12 x 12	20	R	6 x 6	4/0 x 4/0	0.102L,T	1 - 50, 1 - 75
14 x 14	16	L	None	None	0.0	1 - 50
14 x 14	16	L	6 x 12	No. 2 x No. 1	0.072L, 0.056T	1 - 50
14 x 14	16	L	12 x 12	3/0 x 3/0	0.092L,T	1 - 50, 1 - 75
14 x 14	16	L	6 x 12	1/0 x 2/0	0.099L, 0.077T	1 - 50
				1/0 x 4/0	0.099L, 0.109T	1 - 50, 1 - 75
				3/0 x 4/0	0.138L, 0.109T	2 - 50
14 x 14	16	L	12 x 12	7/0 x 7/0	0.169L,T	1 - 50
14 x 14	16	R	12 x 12	3/0 x 3/0	0.092L,T	1 - 50
14 x 14	16	R	6 x 12	1/0 x 4/0	0.099L, 0.109T	1 - 50
14 x 14	20	R	6 x 12	2/0 x 4/0	0.098L, 0.087T	1 - 50

[a] L = Bridgeport crushed limestone coarse aggregate and Trinity River sand from Texas.
R = river gravel and sand from Southern California.

[b] Welded wire sizes shown are steel wire gauge designations.

[c] Steel percentage = steel wire cross-sectional area divided by the total cross-sectional area of the concrete multiplied by 100.

[d] Storage humidities were 50% and 75% RH, both at 73°F.

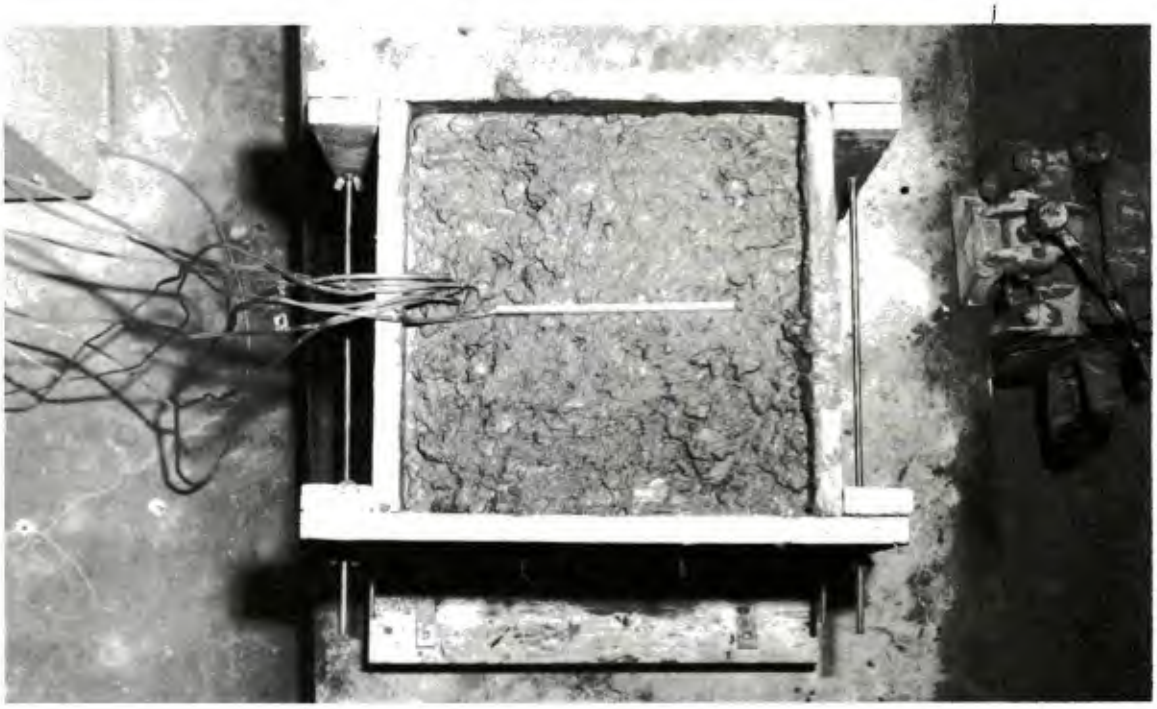

Figure 3. Typical embeddable strain gage.

Figure 4. Prismatic slab-type specimens being cured.

Shrinkage Environments

Following the 28-day curing period during which concrete expansion and concrete precompression due to steel restraint were obtained, the prisms were exposed to drying shrinkage and loss of precompression in either 50% relative humidity (RH) or 75% RH, both at 73°F, for a total period of 365 days.

Strength Properties

Cylinders and beams were made with expansive concretes used in the test program to establish compressive and flexural strengths as well as Young's moduli.

Concrete Mix Design

The concrete mix design used in this study was FAA Class A Paving Concrete (Ref 3), which utilizes 5.8 bags of cement per cubic yard (545 lb) and 5% to 7% air entrainment.

Aggregates

Two high quality aggregates were used in this study: (1) Bridgeport crushed limestone coarse aggregate and Trinity River sand from Texas used in construction of Dallas-Fort Worth Airport, and (2) river gravel and sand from Southern California. All aggregates conformed to gradations specified by FAA (Ref 3). Maximum size of coarse aggregate was 1-1/2 inches.

Cements

The shrinkage-compensating cements used in this study were ChemComp® (ACI Designated Type K), made by two of the five companies licensed to produce the cement. Mortar bar expansions (Ref 4) after 7 days averaged 420 microstrain (0.042%) and 590 microstrain (0.059%) for these two cements. A new standard for expansion of shrinkage-compensating concrete has recently been adopted by ASTM (Ref 5).

Concrete Strengths

Flexural strengths of shrinkage-compensating concretes used in this study averaged 750 psi and 800 psi for 28- and 90-day ages, respectively;

---

3. Federal Aviation Administration Advisory Circular 150/5370-10, Standards for Specifying Construction of Airports, October 24, 1974, p. 332.
4. American Society for Testing and Materials. Standard Test Method for Restrained Expansion of Expansive Cement Mortar, ASTM C806-75.
5. _____. Standard Test Method for Restrained Expansion of Shrinkage-Compensating Concrete, ASTM C878-78, Vol. 14, 1978, pp. 547-550.

corresponding Young's moduli and compressive strength were 4.0×10^6 and 4.2×10^6 psi and 5,180 and 6,030 psi, respectively.

Temperature Effects

In addition to being instrumented with strain gages, one of the 14 by 14-inch prisms 16 inches thick contained thermocouples placed at the following depths, measured from the top: 5, 8, and 12 inches. After 1 year of shrinkage in 50% RH, this prism was subjected to heating tests and to cooling tests to determine these thermal effects upon residual concrete compressive strains.

TEST RESULTS

Concrete Expansion

As indicated above, two different Type K cements were used in this study. One of the two cements provided an average of 38% more expansion during the curing period than did the other. Since, ordinarily, higher expansion means higher induced compressive stresses, the results presented below are those with the cement having the higher expansion only. Differences in shrinkage strains of the two concretes were found to be insignificant.

As indicated in Table 1, 53 prisms of four different thicknesses and with several different levels of reinforcement were involved in the program. At the outset, it was decided to have many different steel percentages rather than to have multiple prisms at just a few steel percentages. In only a few cases were two prisms constructed with the same parameters. Four prisms were made with no steel reinforcing in order to establish the unrestrained expansions for the four different prism thicknesses.

Close examination of all expansion data revealed that the depth of the steel from the top did not significantly affect the magnitude of the concrete expansion strains at any given depth from the top. In other words, for a given steel percentage, whether the steel was at 4 inches from the top (as in a prism 12 inches thick) or 6 inches from the top (as in a prism 20 inches thick), the concrete expansion strains at the measured depths had the same order of magnitude. For this reason, concrete expansion strains at several depths from the top, shown in Figure 5, apply irrespective of the prism thickness (or depth of steel). Least-squares lines were calculated for each depth from the top surface. Least-squares expansion strains from Figure 5 were used to establish the strain-depth relationships shown in Figure 6. Curves similar to those in Figure 6 were constructed for all of the steel percentages at 0.01% intervals between 0.05% and 0.17% as well as for 0%. As indicated in Figure 5(d), expansion strains for the top surface of the prisms were obtained by extrapolation. The influence of the concrete mass is evidenced by the decrease in expansion strains from the free top surface toward the bottom. Another contributing factor to higher expansion strains in the top portion is that the wet burlap applied to the top

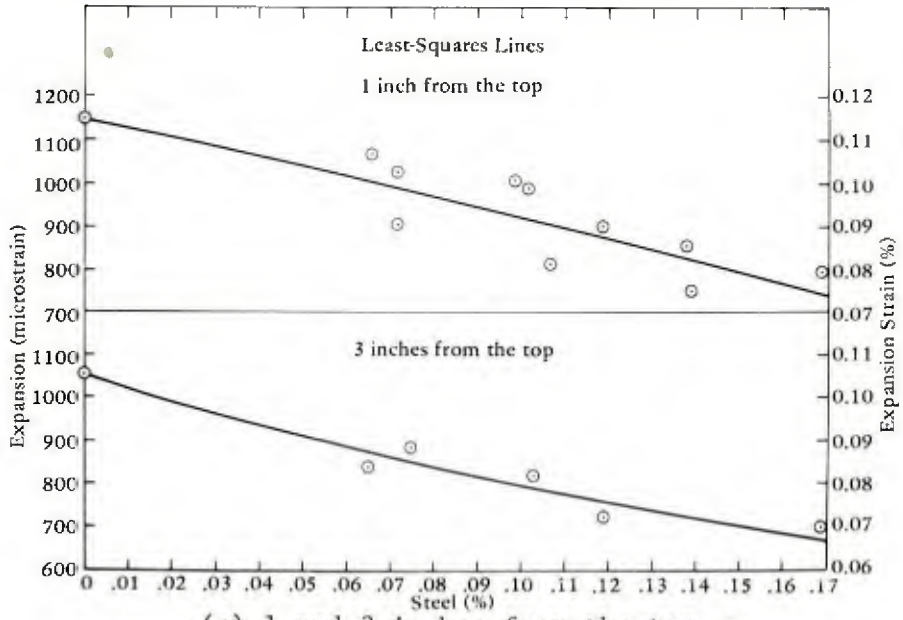

(a) 1 and 3 inches from the top.

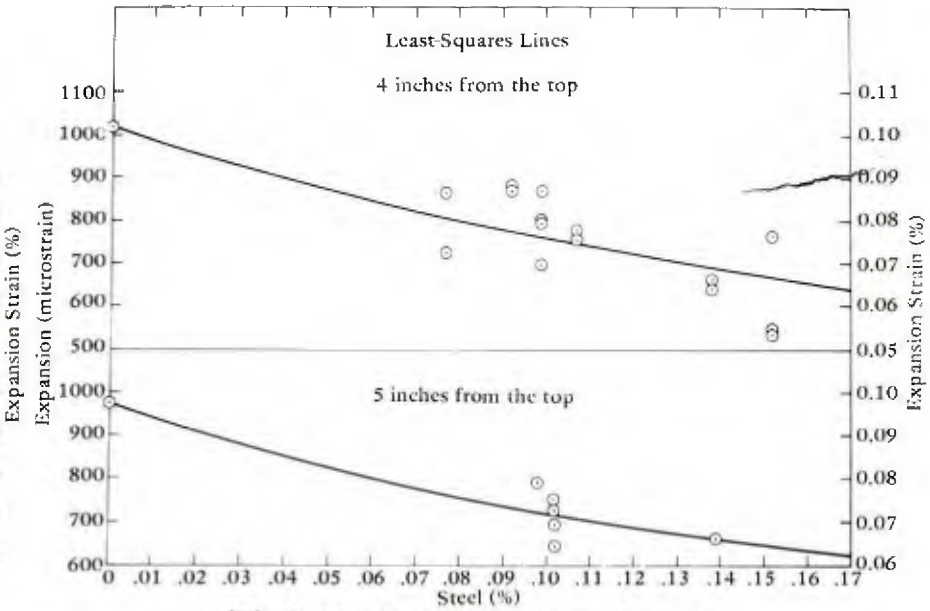

(b) 4 and 5 inches from the top.

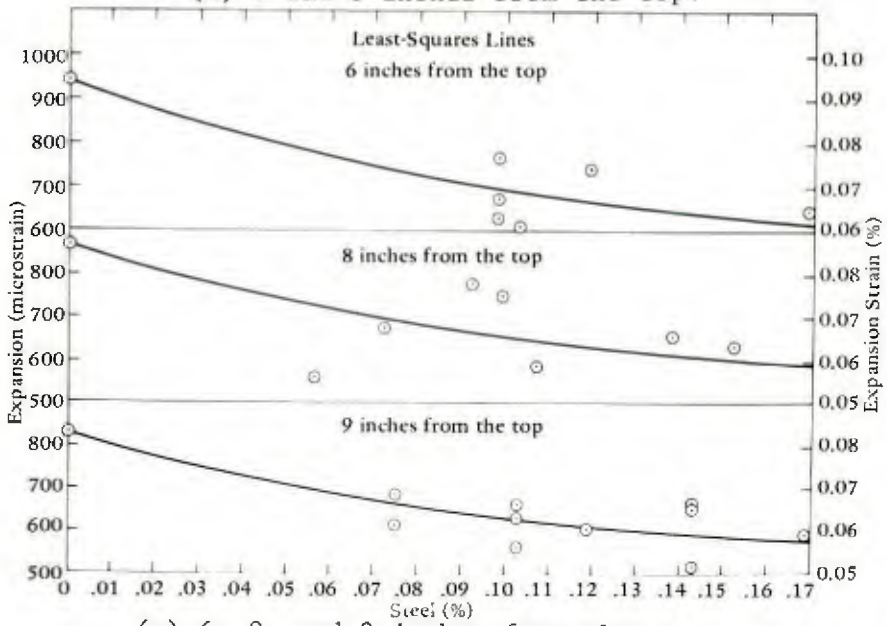

(c) 6, 8, and 9 inches from the top.

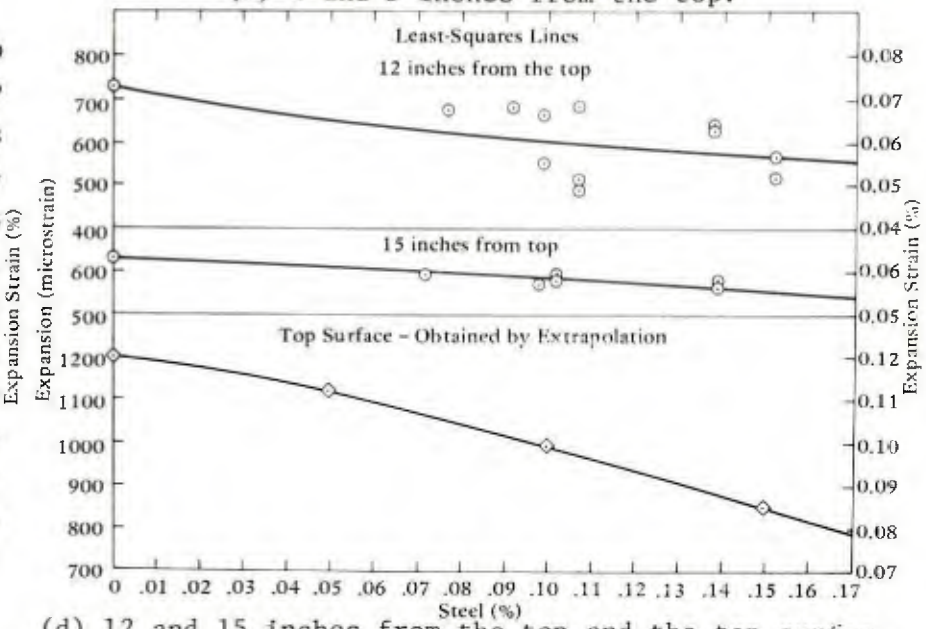

(d) 12 and 15 inches from the top and the top surface.

Figure 5. Concrete expansion strains after 28 days of curing.

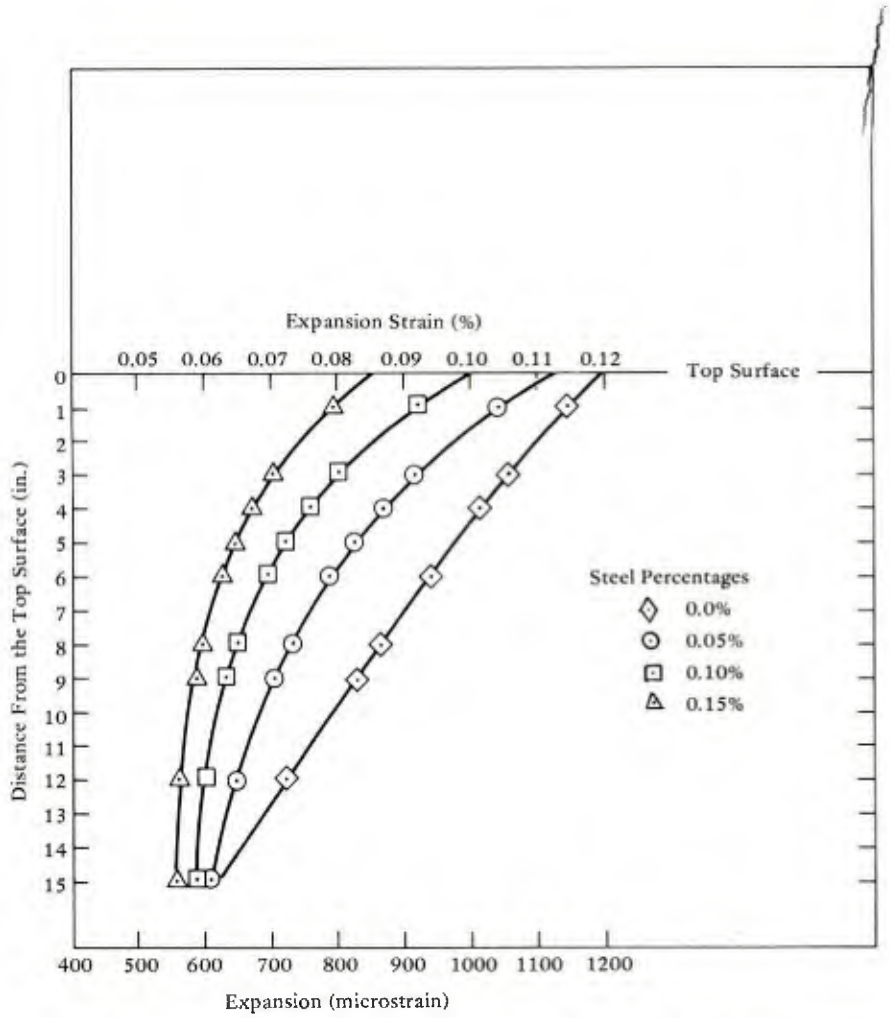

Figure 6. Expansion strain after 28-day curing as a function of depth from top surface for selected steel percentages.

surface provided better curing conditions, thus more expansion. Concrete expansion strains for all pertinent steel percentages and depths from the top surface are shown in Table 2.

In reinforced expansive concrete, compressive stresses induced by concrete expansion are calculated as follows (Ref 6):

$$\text{Average stress in concrete } (f_c) = \varepsilon_c \times \frac{A_s}{A_c} \times E_s = \varepsilon_c \times p \times E_s$$

where ε_c = expansion strain in the concrete

E_s = Young's modulus of the steel (taken in this report as 29×10^6 psi)

---

6. American Concrete Institute. Recommended Practice for the Use of Shrinkage-Compensating Concrete, ACI Standard 223-77, 1977.

A_s = cross-sectional area of steel

A_c = cross-sectional area of concrete

$A_s/A_c = p$ = steel ratio

For simplicity, it will be assumed that the concrete stresses calculated with the above equation are correct only at the location or depth of the steel. Since the welded wire fabric in this study was at different depths in prisms of different thicknesses, and since concrete strains were not measured at the depth of the steel, it was necessary to determine the concrete expansion strain at the appropriate depths of steel; i.e., at 4, 5, and 6 inches from the top surface. These expansion strains are shown in Table 2.

Since it is the resistance of the steel to the expansion of the concrete which induces the concrete compression, the value of induced concrete compression must be highest at the steel depth and must diminish above and below that depth. On the other hand, for a given steel percentage, the stated equation indicates that as the concrete strain increases, so does the concrete stress. Table 2 shows that for any steel percentage, the expansion strains increase in magnitude above the steel depths of either 4, 5, or 6 inches. Indiscriminate use of the equation with these higher strains would result in higher compressive stresses at the top than at the steel depth, which has already been shown to be incorrect.

The solution to this dilemma involves application of the fundamentals of expansive concretes. If an expansive concrete is unrestrained (contains no steel) and is thus free to expand with no restraint, no concrete compression is induced. In an expansive concrete containing steel, the induced concrete compressive stress is also a function of how much of the "free" or unrestrained expansion the steel prevented from occurring. The expansion strains which the steel prevented from occurring can be calculated from Table 2 by subtracting the expansion strains for a given steel percentage from the unrestrained expansion strains in the steel percentage column headed 0.00. Table 3 is a compilation of these strains. For example, referring to a steel percentage of 0.10% at the top surface in Table 2, the expansion prevented by the steel is 1,190 minus 995 (or 195 microstrain), as shown at the top of the 0.10 column in Table 3. When the strains in Table 3 are divided by the unrestrained expansion strains found in the 0.00 steel percentage column of Table 2, the resulting ratio is a measure of the relative effectiveness of the steel to induce compression in the concrete at a given depth from the top. These ratios are presented in Table 4. For example, for steel percentage of 0.15% and a depth from the top of 4 inches, prevented expansion strain (Table 3) is 340 microstrain, and unrestrained expansion strain for a depth of 4 inches (Table 2) is 1,015 microstrain; the ratio, then, is 340 ÷ 1,015 = 0.33, as shown in Table 4.

Concrete compressive stresses resulting from expansion (induced) are shown in Table 5 for prisms 12, 16, and 20 inches thick. Referring to Table 5(a) for a prism 12 inches thick, the steel is at a depth of 4 inches from the top. As stated above, the concrete stresses at the depth of the steel are computed by using the equation $f_c = \varepsilon_c \times p \times E_s$.

For example, with a steel percentage of 0.15 and a depth of steel of 4 inches, expansion strain from Table 2 is 675 microstrain; then $f_c = (675 \times 10^{-6}) \times (0.0015) \times (29 \times 10^6) = 29$ psi. By the reasoning presented, concrete stresses above and below the steel depth should be lower than those at the steel depth. These stresses are calculated for one steel percentage at a time by dividing the ratio of prevented to unrestrained expansion strain (Table 4) for depths from the top other than the steel depth by the ratio of prevented to unrestrained expansion strain at the steel depth and multiplying by the concrete stress at the steel depth (Table 5). For example, for a steel percentage of 0.15% at a depth of 1 inch from the top, the ratio of prevented to unrestrained expansion (Table 4) = 0.31; the corresponding ratio at a depth of steel of 4 inches is equal to 0.33; according to Table 5(a), the concrete stress at steel depth of 4 inches is equal to 29 psi; then $0.31 \div 0.33 \times 29 = 27$ psi compressive stress as indicated in 0.15 column, 1 inch from top, of Table 5(a).

Examination of Table 5 reveals that the stresses above and below the steel depth are not always lower than the stress at the steel depth, but the analysis and reasoning behind the computations are believed to be sufficiently accurate since the quantitative variations are slight. Determination of realistic transverse joint spacing is dependent upon the residual concrete expansive stresses after all expected losses have occurred.

Steel Expansion

Measured steel expansion strains, due to the unique rectangular rigid shape caused by welding, were rather erratic and varied over rather wide ranges. Results are presented in Appendix B.

Concrete Shrinkage

Following the 28-day curing period, the foil and burlap were removed from the top of each prism and the prism was transferred to a drying environment, either 50% or 75% RH. As indicated in Table 1, most of the prisms were placed in 50% RH because it would cause higher shrinkage strains than the 75% RH and thus would be more severe in terms of reduction of expansion stresses. Typical shrinkage data for a steel percentage of 0.056% are shown in Figure 7 at selected depths from the top surface. As with the expansion strains, the shrinkage strain data versus depth from the top surface were not significantly affected by the depth of the steel; i.e., by the prism thickness. Table 6 is a compilation of the shrinkage strains for prisms with steel percentages of 0.056%, 0.107%, and 0.169%; the quantitative strain differences among the three steel percentages are very slight. Since the shrinkage strains in the prisms with steel percentage of 0.056% are slightly higher than the others near the top surface, these values are used in subsequent calculations. Figure 8 shows shrinkage strains versus depth from the top surface. As with the expansion strains, these curves, together with curves such as those shown in Figure 7, permit the shrinkage strains at the top surface to be determined by extrapolation.

TABLE 2. – CONCRETE EXPANSION STRAINS AFTER 28 DAYS OF CURING

Depth From Top, in.	Strains (microstrain) for Steel Percentages of —													
	0.00	0.05	0.06	0.07	0.08	0.09	0.10	0.11	0.12	0.13	0.14	0.15	0.16	0.17
0	1,190[a]	1,120[a]	1,095[a]	1,070[a]	1,045[a]	1,020[a]	995[a]	965[a]	935[a]	910[a]	880[a]	850[a]	820[a]	790[a]
1	1,145	1,040	1,020	995	970	945	920	895	870	845	820	795	770[a]	740[a]
2	1,100	975	950	925	905	880	855	835	810	790	770	745	725[a]	705[a]
3	1,055	915	890	865	845	825	800	780	760	740	725	705	685[a]	670[a]
4	1,015	870	845	820	800	780	760	740	725	705	690	675	660[a]	645[a]
5	975	825	805	780	760	740	725	705	690	675	665	650	635[a]	625[a]
6	940	790	765	745	725	710	695	675	665	650	640	630	620[a]	610[a]
7	900	760	735	720	700	685	670	655	650	635	625	615	605[a]	595[a]
8	865	735	715	695	680	665	650	640	630	620	610	600	590[a]	585[a]
9	830	705	690	670	660	645	635	625	615	605	600	590	585[a]	575[a]
10	795	685	670	655	645	635	620	615	605	600	590	580	575[a]	570[a]
11	760	665	650	640	630	625	610	605	595	590	580	570	565[a]	565[a]
12	725	650	640	630	620	615	605	600	590	585	575	565	560[a]	555[a]
13	695[a]	635	625	620	610	605	595	595	585	580	575	565	560[a]	555[a]
14	660[a]	625	615	610	605	600	595	590	580	575	570	560	555[a]	550[a]
15	630[a]	610	605	605	600	595	590	585	575	570	570	560	555[a]	550[a]

[a]These expansion strains were obtained by extrapolation.

TABLE 3. – CONCRETE EXPANSION STRAINS PREVENTED BY THE STEEL

Depth From Top, (in.)	Strains[a] (microstrain) for Steel Percentages of —												
	0.05	0.06	0.07	0.08	0.09	0.10	0.11	0.12	0.13	0.14	0.15	0.16	0.17
0	70	95	120	145	170	195	225	255	280	310	340	370	400
1	105	125	150	175	200	225	250	275	300	325	350	375	405
2	125	150	175	195	220	245	265	290	310	330	355	375	395
3	140	165	190	210	230	255	275	295	315	330	350	370	385
4	145	170	195	215	235	255	275	290	310	325	340	355	370
5	150	170	195	215	235	250	270	285	300	310	325	340	350
6	150	175	195	215	230	245	265	275	290	300	310	320	330
7	140	165	180	200	215	230	245	250	265	275	285	295	305
8	130	150	170	185	200	215	225	235	245	255	265	275	280
9	125	140	160	170	185	195	205	215	225	230	240	245	255
10	110	125	140	150	160	175	180	190	195	205	215	220	225
11	95	110	120	130	135	150	155	165	170	180	190	195	195
12	75	85	95	105	110	120	125	135	140	150	160	165	170
13	60	70	75	85	90	100	100	110	115	120	130	135	140
14	35	45	50	55	60	65	70	80	85	90	100	105	110
15	20	25	25	30	35	40	45	55	60	60	70	75	80

[a]Obtained from Table 2 by subtracting the expansion strains for a given steel percentage and depth from the top from the unrestrained expansion (steel percentage = 0.0) at the same depth; example: for a depth of 4 inches from the top, unrestrained expansion = 1,015 microstrain (Table 2) and for p = 0.15%, the expansion strain = 675 microstrain (Table 2); then the expansion prevented by the steel = 1,015 minus 675 = 340 microstrain.

TABLE 4. –RATIO OF PREVENTED EXPANSION TO UNRESTRAINED EXPANSION

Depth From Top, in.	Ratios[a] for Steel Percentages of —												
	0.05	0.06	0.07	0.08	0.09	0.10	0.11	0.12	0.13	0.14	0.15	0.16	0.17
0	0.06	0.08	0.10	0.12	0.14	0.16	0.19	0.21	0.24	0.26	0.29	0.31	0.34
1	0.09	0.11	0.13	0.15	0.17	0.20	0.22	0.24	0.26	0.28	0.31	0.33	0.35
2	0.11	0.14	0.16	0.18	0.20	0.22	0.24	0.26	0.28	0.30	0.32	0.34	0.36
3	0.13	0.16	0.18	0.20	0.22	0.24	0.26	0.28	0.30	0.32	0.33	0.35	0.36
4	0.14	0.17	0.19	0.21	0.23	0.25	0.27	0.29	0.31	0.32	0.33	0.35	0.36
5	0.15	0.17	0.20	0.22	0.24	0.26	0.28	0.29	0.31	0.32	0.33	0.35	0.36
6	0.16	0.19	0.21	0.23	0.24	0.26	0.28	0.29	0.31	0.32	0.33	0.34	0.35
7	0.16	0.18	0.20	0.22	0.24	0.26	0.27	0.28	0.29	0.31	0.32	0.33	0.34
8	0.15	0.17	0.20	0.21	0.23	0.25	0.26	0.27	0.28	0.29	0.31	0.32	0.32
9	0.15	0.17	0.19	0.20	0.22	0.23	0.25	0.26	0.27	0.28	0.29	0.30	0.31
10	0.14	0.16	0.18	0.19	0.20	0.22	0.23	0.24	0.25	0.26	0.27	0.28	0.28
11	0.12	0.14	0.16	0.17	0.18	0.20	0.20	0.22	0.22	0.24	0.25	0.26	0.26
12	0.10	0.12	0.13	0.14	0.15	0.17	0.17	0.19	0.19	0.21	0.22	0.23	0.23
13	0.09	0.10	0.11	0.12	0.13	0.14	0.14	0.16	0.17	0.17	0.19	0.19	0.20
14	0.05	0.07	0.08	0.08	0.09	0.10	0.11	0.12	0.13	0.14	0.15	0.16	0.17
15	0.03	0.04	0.04	0.05	0.06	0.06	0.07	0.09	0.10	0.10	0.11	0.12	0.13

[a] Obtained by dividing the prevented expansion strain in Table 3 by the corresponding unrestrained expansion strain (p = 0.0%) in Table 2; example: for p = 0.15% and depth from top of 4 inches, prevented expansion strain = 340 microstrain (Table 3), unrestrained expansion strain = 1,015 microstrain (Table 2), then ratio = 340 divided by 1,015 = 0.33.

TABLE 5. - CONCRETE COMPRESSIVE STRESSES DUE TO EXPANSION

Depth From Top, in.	Stresses[a] (psi) for Steel Percentages of –												
	0.05	0.06	0.07	0.08	0.09	0.10	0.11	0.12	0.13	0.14	0.15	0.16	0.17
(a) For prism 12 inches thick with steel 4 inches from top													
0	6	7	9	11	12	14	17	18	21	23	25	27	30
1	8	10	12	14	15	18	20	21	23	24	27	29	31
2	10	12	14	16	17	19	21	22	24	26	28	30	32
3	12	14	16	18	19	21	23	24	26	28	29	31	32
4	13	15	17	19	20	22	24	25	27	28	29	31	32
5	14	15	18	20	21	23	25	25	27	28	29	31	32
6	14	17	19	21	21	23	25	25	27	28	29	30	31
7	14	16	18	20	21	23	24	24	25	27	28	29	30
8	14	15	18	19	20	22	23	23	24	25	27	28	28
9	14	15	17	18	19	20	22	22	24	24	25	27	28
10	13	14	16	17	17	19	20	21	22	23	24	25	25
11	11	12	14	15	16	18	18	19	19	21	22	23	23
12	9	11	12	13	13	15	15	16	17	18	19	20	20
(b) For prism 16 inches thick with steel 5 inches from top													
0	4	7	8	10	11	13	15	17	19	22	25	26	29
1	7	9	10	12	13	16	17	20	21	24	26	27	30
2	9	12	13	15	16	18	19	22	23	25	27	28	31
3	10	12	14	16	17	19	20	23	24	27	28	29	31
4	11	14	15	17	18	20	21	24	25	27	28	29	31
5	12	14	16	18	19	21	22	24	25	27	28	29	31
6	13	16	17	19	19	21	22	24	25	27	28	28	30
7	13	15	16	18	19	21	21	23	23	26	27	27	29
8	12	14	16	17	18	20	20	22	23	24	26	27	28
9	12	14	15	16	17	19	20	22	22	24	25	25	27
10	11	13	14	16	16	18	18	20	20	22	23	23	24
11	10	12	13	14	14	16	16	18	18	20	21	22	22
12	8	10	10	11	12	14	13	16	15	18	19	19	20
13	7	8	9	10	10	11	11	13	14	14	16	16	17
14	4	6	6	7	7	8	9	10	10	12	13	13	15
15	2	3	3	4	5	5	6	7	8	8	9	10	11

Depth From Top, in.	Stresses[a] (psi) for Steel Percentages of –												
	0.05	0.06	0.07	0.08	0.09	0.10	0.11	0.12	0.13	0.14	0.15	0.16	0.17
(c) For prism 20 inches thick with steel 6 inches from top													
0	4	6	7	9	10	12	15	17	19	21	24	26	29
1	6	8	9	11	13	15	17	19	20	23	25	28	30
2	8	10	11	13	15	17	19	21	22	24	26	29	31
3	9	12	13	15	16	18	20	22	23	26	27	30	31
4	10	13	14	16	17	19	21	23	24	26	27	30	31
5	10	13	14	16	18	20	22	23	24	26	27	30	31
6	11	14	15	17	18	20	22	23	24	26	27	29	30
7	11	13	14	16	18	20	21	22	22	25	26	28	29
8	10	13	14	16	17	19	20	21	22	24	25	27	27
9	10	13	14	15	16	18	20	21	21	23	24	26	27
10	10	12	13	14	15	17	18	19	19	21	22	24	24
11	8	10	11	13	14	15	16	17	17	20	20	22	22
12	7	9	10	10	11	13	13	15	15	17	19	20	20
13	6	7	8	9	10	11	11	13	13	14	16	16	17
14	3	5	6	6	8	8	9	10	10	11	12	14	15
15	2	3	3	4	4	5	6	7	8	8	9	10	11

[a]Stresses were calculated as follows: (a) For concrete stress at the steel depth, obtain the expansion strain from Table 2 and then $f_c = \epsilon_c \times p \times E_s$; example: for p = 0.15% and steel depth of 4 inches (prism 12 inches thick), expansion strain = 675 microstrain (Table 2), then $f_c = (675 \times 10^{-6}) \times (0.0015) \times (29 \times 10^6) = 29$ psi; (b) To obtain stresses for other than the steel depth: for a given steel percentage, divide the ratio of prevented to unrestrained expansion for depths other than the steel depth (Table 4) by the ratio of prevented to unrestrained expansion for the steel depth and multiply by the concrete stress at the steel depth calculated under (a) above; example: for Table 5(a) – prism 12 inches thick with steel at 4 inches from the top – at p = 0.15% and for a depth of 1 inch from the top, ratio of prevented to unrestrained expansion = 0.31 (Table 4), ratio of prevented to unrestrained expansion at a steel depth of 4 inches = 0.33 (Table 4), calculated concrete stress at steel depth of 4 inches = 29 psi (see (a) above); then concrete stress for p = 0.15% and depth of 1 inch = 0.31 divided by 0.33 and multiplied by 29 = 27 psi.

TABLE 6. - SHRINKAGE STRAINS IN 50% RH

Depth From Top, in.	Shrinkage Strains (microstrain) for –											
	50 Days			100 Days			200 Days			365 Days		
	With Steel Percentages of –											
	0.056	0.107	0.169	0.056	0.107	0.169	0.056	0.107	0.169	0.056	0.107	0.169
0	130	134	131	167	165	161	179	175	171	183	180	175
1	112	117	118	143	144	144	154	153	153	158	157	157
2	97	104	107	126	128	130	136	137	139	140	141	142
3	86	92	96	112	115	118	121	124	126	125	127	129
4	75	82	87	101	103	107	110	111	114	113	115	117
5	67	74	78	91	93	96	99	101	103	102	104	107
6	60	66	70	82	84	87	90	91	94	92	94	97
7	53	58	63	73	75	78	81	82	85	83	85	88
8	47	51	55	66	67	70	73	74	76	75	77	79
9	41	45	48	59	60	61	65	66	68	68	69	72
10	37	39	42	52	52	55	58	58	60	61	61	63
11	32	33	36	46	45	47	52	50	52	54	53	55
12	28	29	29	40	39	40	44	44	45	47	46	47
13	24	23	23	34	32	33	39	37	37	41	39	40
14	21	18	17	29	26	26	32	30	30	34	33	32
15	17	13	12	23	20	20	26	24	23	28	26	25

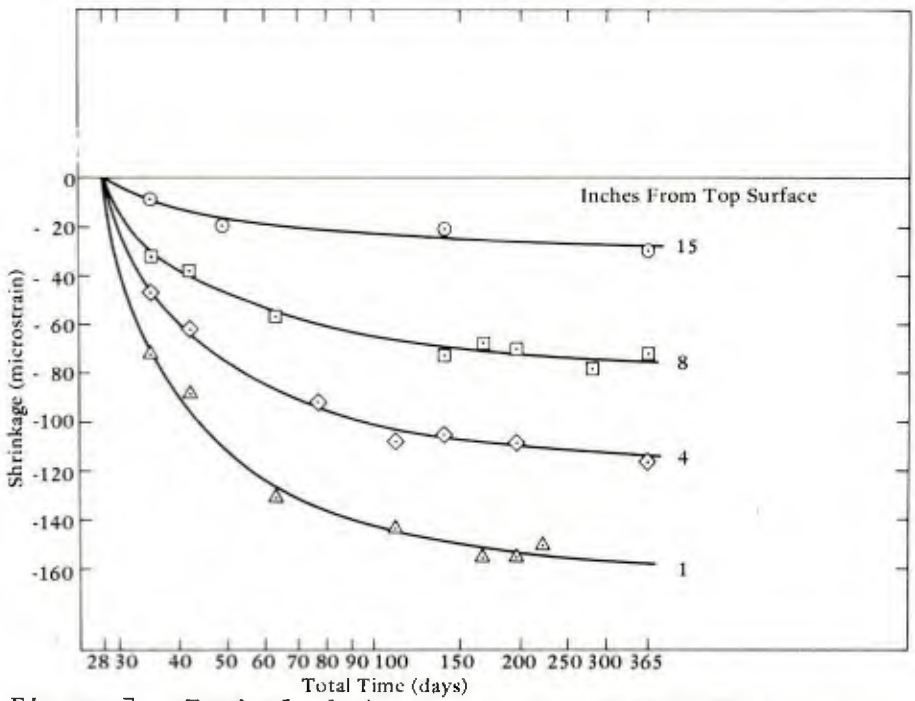

Figure 7. Typical shrinkage strains in 50% RH with steel percentage of 0.056%.

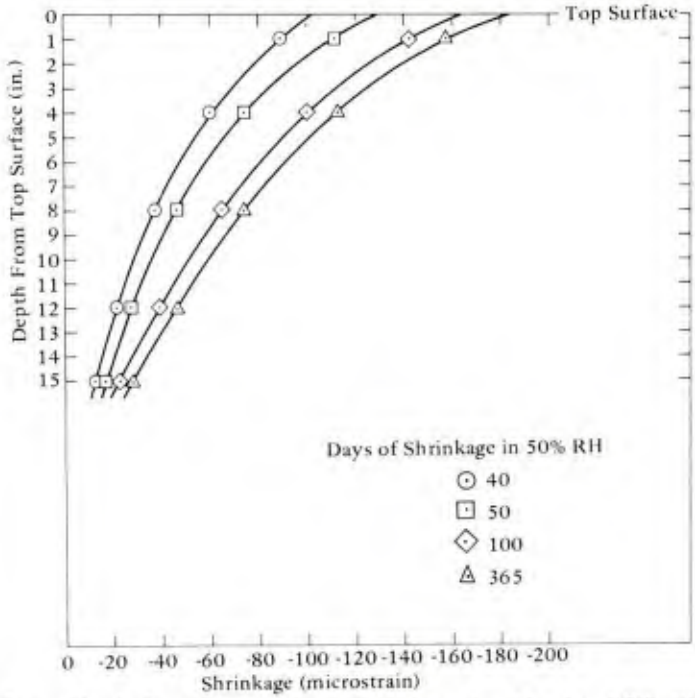

Figure 8. Shrinkage strains versus depth in 50% RH for prisms with steel percentage of 0.056%.

Residual expansion strains after shrinkage for 365 days in 50% RH are presented in Table 7. Residual compressive stresses are shown in Table 8 for prism thicknesses of 12, 16, and 20 inches. Computation of the stresses at the steel depth is by the equation $f_c = \varepsilon_c \times p \times E_s$, as before; the residual strains shown in Table 7 at steel depths of 4, 5, and 6 inches are used to calculate the corresponding stresses at the steel depth for Table 8(a), (b), and (c). Stresses at depths other than steel depth are obtained by multiplying the residual stress at the steel depth by the ratio of the residual strain after shrinkage to the expansion strain at corresponding depths and steel percentages. For example, for a prism 12 inches thick with steel at 4 inches from the top, the residual strain for a steel percentage of 0.15% and 1 inch from the top is 637 microstrain (Table 7); the corresponding concrete expansive strain is 795 microstrain (Table 2); corresponding concrete expansive stress from Table 5(a) is 27 psi; then residual compressive stress at 1 inch from the top surface with steel percentage of 0.15% is 637 ÷ 795 x 27 = 22 psi, as shown in Table 8(a). Comparisons of stresses in Table 5 and Table 8 indicate that shrinkage after 365 days in 50% RH causes a maximum concrete compressive stress loss of only 7 psi at the top surface with a steel percentage of 0.17%; most other losses are less than 7 psi.

Typical shrinkage data obtained in 75% RH are shown in Figure 9 for three different depths from the top. Since shrinkage strains in 75% RH are not as high as in 50% RH and, therefore, would not reduce the induced compressive stresses as much, no attempt was made to calculate residual concrete stresses in 75% RH. On the average, shrinkage strains in 75% RH were about 37% less than those in 50% RH ($S_{75} = 0.63\ S_{50}$).

TABLE 7. - RESIDUAL EXPANSION STRAINS AFTER SHRINKAGE FOR 365 DAYS IN 50% RH

Depth From Top, in.	Strains[a] (microstrain) for Steel Percentages of –												
	0.05	0.06	0.07	0.08	0.09	0.10	0.11	0.12	0.13	0.14	0.15	0.16	0.17
0	937	912	887	862	837	812	782	752	727	697	667	637	607
1	882	862	837	812	787	762	737	712	687	662	637	612	582
2	835	810	785	765	740	715	695	670	650	630	605	585	565
3	790	765	740	720	700	675	655	635	615	600	580	560	545
4	757	732	707	687	667	647	627	612	592	577	562	547	532
5	723	703	678	658	638	623	603	588	573	563	548	533	523
6	698	673	653	633	618	603	583	573	558	548	538	528	518
7	677	652	637	617	602	587	572	567	552	542	532	522	512
8	660	640	620	605	590	575	565	555	545	535	525	515	510
9	637	622	602	592	577	567	557	547	537	532	522	517	507
10	624	609	594	584	574	559	554	544	539	529	519	514	509
11	611	596	586	576	571	556	551	541	536	526	516	511	511
12	603	593	583	573	568	558	553	543	538	528	518	513	508
13	594	584	579	569	564	554	554	544	539	534	524	519	514
14	591	581	576	571	566	561	556	546	541	536	526	521	516
15	582	577	577	572	567	562	557	547	542	542	532	527	522

[a]Obtained by subtracting 365-day shrinkage strains for p = 0.056% in Table 6 from corresponding expansion strains in Table 2; example: for the 0 depth-from-top line in Table 7, the 365-day shrinkage strain of 183 microstrain on the 0 depth line in Table 6 is subtracted from each of the 0-depth expansion strains in Table 2; for p = 0.07%, residual expansion strain = 1,070 (Table 2) minus 183 (Table 6) = 887 microstrain.

TABLE 8. - RESIDUAL CONCRETE COMPRESSIVE STRESSES AFTER SHRINKAGE FOR 365 DAYS IN 50% RH

Depth From Top, in.	Stresses[a] (psi) for Steel Percentages of –												
	0.05	0.06	0.07	0.08	0.09	0.10	0.11	0.12	0.13	0.14	0.15	0.16	0.17
(a) For prism 12 inches thick with steel 4 inches from top													
0	5	6	7	9	10	11	14	14	17	18	20	21	23
1	7	8	10	12	12	15	16	17	19	19	22	23	24
2	9	10	12	14	14	16	17	18	20	21	23	24	26
3	10	12	14	15	16	18	19	20	22	23	24	25	26
4	11	13	14	16	17	19	20	21	22	23	24	25	26
5	12	13	16	17	18	20	21	21	23	24	24	26	27
6	12	15	17	18	18	20	22	22	23	24	25	26	26
7	12	14	16	18	18	20	21	21	22	23	24	25	26
8	13	13	16	17	18	19	20	20	21	22	24	24	24
9	13	14	15	16	17	18	20	20	21	21	22	24	25
10	12	13	14	15	15	17	18	19	20	21	21	22	22
11	10	11	13	14	15	16	16	17	17	19	20	21	21
12	8	10	11	12	12	14	14	15	16	17	17	18	18
(b) For prism 16 inches thick with steel 5 inches from top													
0	3	6	7	8	9	11	12	14	15	17	20	20	22
1	6	8	8	10	11	13	14	16	17	19	21	21	24
2	8	10	11	13	13	15	16	18	19	20	22	23	25
3	9	10	12	14	14	16	17	19	20	22	23	24	25
4	10	12	13	15	15	17	18	20	21	23	23	24	26
5	10	12	14	15	17	18	19	20	22	23	24	25	26
6	11	14	15	17	17	18	19	21	21	23	24	24	25
7	12	13	14	16	17	18	18	20	20	23	23	23	25
8	11	13	14	15	16	18	18	19	20	21	23	24	24
9	11	13	13	14	15	17	18	20	20	21	22	22	24
10	10	12	13	14	14	16	16	18	18	20	21	21	21
11	9	11	12	13	13	15	15	16	16	18	19	20	20
12	7	9	9	10	11	13	12	15	14	17	17	17	18
13	7	7	8	9	9	10	10	12	13	13	15	15	16
14	4	6	6	7	7	8	8	9	9	11	12	12	14
15	2	3	3	4	5	5	6	7	8	8	9	9	10

Depth From Top in.	Stresses[a] (psi) for Steel Percentages of –												
	0.05	0.06	0.07	0.08	0.09	0.10	0.11	0.12	0.13	0.14	0.15	0.16	0.17
(c) For prism 20 inches thick with steel 6 inches from top													
0	3	5	6	7	8	10	12	14	15	17	19	20	22
1	5	7	8	9	11	12	14	16	16	19	20	22	24
2	7	9	9	11	13	14	16	17	18	20	21	23	25
3	8	10	11	13	14	15	17	18	19	22	22	25	25
4	9	11	12	14	15	16	18	19	20	22	22	25	26
5	9	11	12	14	16	17	19	20	20	22	23	25	26
6	10	12	13	15	16	17	19	20	21	22	23	24	26
7	10	12	12	14	16	18	18	19	19	22	22	24	25
8	9	12	12	14	15	17	18	18	19	21	22	24	24
9	9	12	13	13	14	16	18	19	19	20	21	23	24
10	9	11	12	13	14	15	16	17	17	19	20	21	21
11	7	9	10	12	13	14	15	15	15	18	18	20	20
12	6	8	9	9	10	12	12	14	14	16	17	18	18
13	6	7	7	9	9	10	10	12	12	13	15	15	16
14	3	5	6	6	8	8	8	9	9	10	11	13	14
15	2	3	3	4	4	5	6	7	8	8	9	9	10

[a]Stresses were calculated as follows: (a) For concrete stress at the steel depth, obtain the residual expansion strain after shrinkage in 50% RH from Table 7, then $f_c = \epsilon_c \times p \times E_s$; example: for p = 0.15% and steel depth of 4 inches (prism 12 inches thick), residual expansion strain after shrinkage in 50% RH = 562 microstrain (Table 7); then, $f_c = (562 \times 10^{-6}) \times (0.0015) \times (29 \times 10^6) =$ 24 psi; (b) To obtain stresses for other than the steel depth: for a given steel percentage, divide the residual concrete strain after shrinkage in 50% RH (Table 7) by the corresponding expansion strain (Table 2) and multiply by the corresponding expansion stress (Table 5); example: for Table 8(a) – prism 12 inches thick with steel at 4 inches from the top – with p = 0.15% at a depth of 1 inch from the top, residual expansion strain after shrinkage in 50% RH = 637 microstrain (Table 7), concrete expansion strain = 795 microstrain (Table 2), and concrete expansion stress = 27 psi (Table 5a); then 637 divided by 795 x 27 = 21.6 or 22 psi.

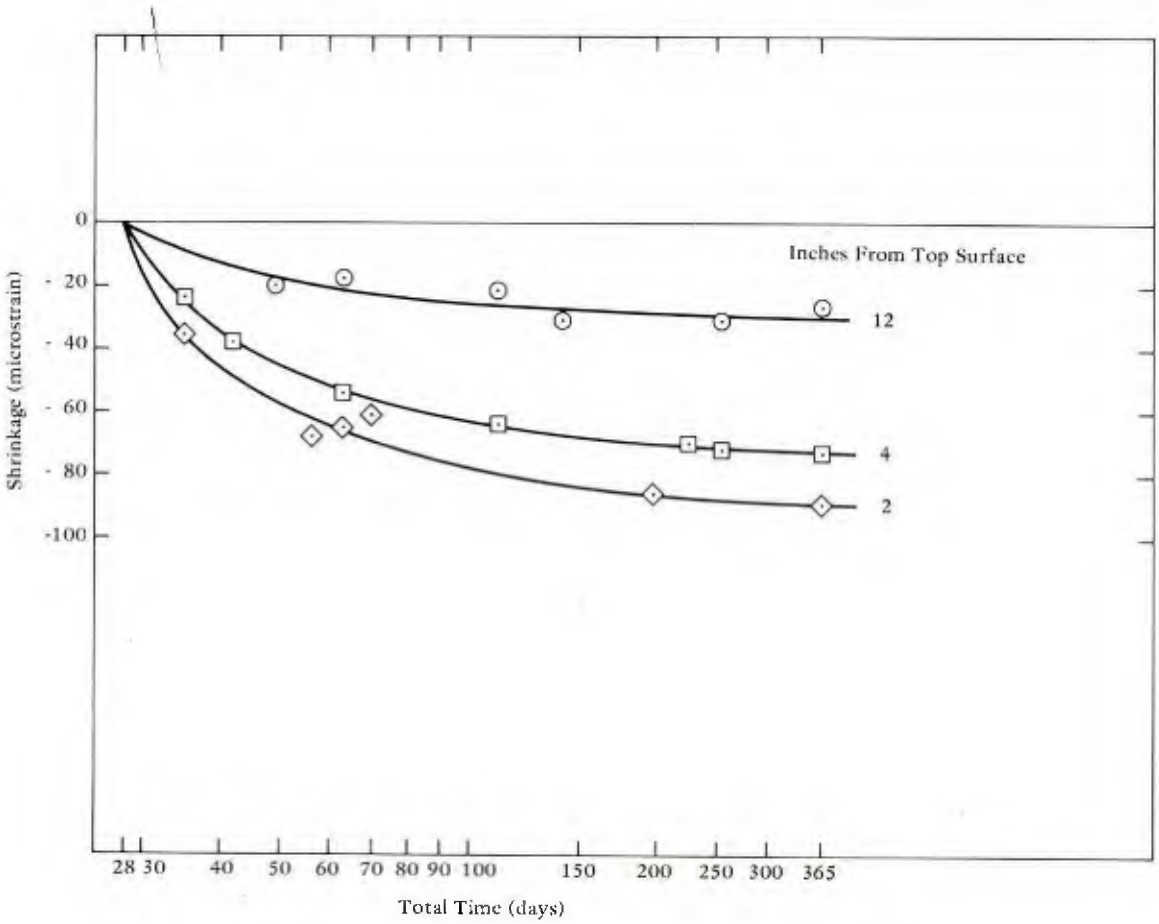

Figure 9. Typical shrinkage strains in 75% RH.

Comprehensive concrete shrinkage studies have been conducted at CEL (Ref 7-10) which involved large, medium, and small specimens of various shapes, reinforced as well as nonreinforced, exposed in drying environments from 20% RH to 100% RH. These studies revealed that shrinkage is a function of the ratio of the exposed surface area to the volume. From these previous studies, with prismatic specimens of the type used in this

7. Naval Civil Engineering Laboratory. Technical Report R-333-I, Study of Creep in Concrete, Phase 1, by John R. Keeton, Port Hueneme, CA, 15 Jan 1965.
8. _____. Technical Report R-333-III, Study of Creep in Concrete, Phases 3, 4, and 5, by John R. Keeton, Port Hueneme, CA, May 1965.
9. _____. Technical Report R-704, Creep and Shrinkage of Reinforced Thin-Shell Concrete, by John R. Keeton, Port Hueneme, CA, Nov 1970.
10. _____. Technical Note N-1504, Expansive Cement Concretes for Naval Construction, by John R. Keeton, Port Hueneme, CA, Nov 1977.

study, shrinkage strains in 20% RH averaged about 30% more than those in 50% RH ($S_{20} = 1.3\ S_{50}$). Applying this ratio to the 365-day shrinkage strains for p = 0.056% in Table 6 results in the last column of Table 9. The rest of the strains in Table 9 were calculated by subtracting the strains in the last column of the table from the corresponding expansion strains in Table 2. For example, for a steel percentage of 0.15% at 2 inches from the top, expansion strain from Table 2 is 745 microstrain and shrinkage in 20% RH is 182 microstrain (last column of Table 9); then residual expansion strain after shrinkage for 365 days in 20% RH is 745 minus 182, which is 563 microstrain.

Residual concrete compressive stresses after 365 days of shrinkage in 20% RH are shown in Table 10 for prisms 12, 16, and 20 inches thick. Stresses in Table 10 were calculated in the same manner as those in Table 8, using the 20% RH shrinkage strain in Table 9 rather than the 50% RH shrinkage strain in Table 6. Examination of Table 10 reveals that after 1 year of shrinkage in 20% RH, the concrete still retains most of its precompression.

Combining the shrinkage data obtained in this study with those of previous studies enables construction of Figure 10, shrinkage strains for humidities from 20% through 100% RH. Since the curves meet at zero for 100% RH, they should be recognized as conservative in the humidity range from 75% to 100% RH, because the swellage (absorption) from 96% through 100% RH actually lowers the curves slightly in that area. A compilation of shrinkage versus humidity is shown in Table 11.

Thermal Studies - Cooling

One of the prisms 14 inches square and 16 inches thick with steel percentage of 0.092 was instrumented with thermocouples in addition to embedded strain gages. Thermocouples were placed at 5, 8, and 12 inches from the top; embedded strain gages were located 4, 8, and 12 inches from the top; steel was 5 inches from the top. To simulate to some degree the effect of a large mass of adjoining concrete, 3 inches of polyurethane foam board stock was placed on all four sides of the prism, leaving the top exposed to subsequent cooling and heating tests. This prism had been in 50% RH for over 1 year prior to thermal testing.

Results of the cooling tests are presented in Figure 11. The prism, stabilized at ambient indoor temperatures for several days, was placed in the CEL cold chamber before the chamber was turned on; cooling to the set temperature of 10°F required about 6 hours. The first data points shown in Figure 11 are 6-hour readings.

At the beginning of cooling, cumulative temperature differences at 5 inches from the top, as expected, were slightly higher than the others, but after 72 hours the differences at all three depths were about the same. Cumulative concrete strain differences at 4 inches from the top were higher than the others from the beginning of cooling through about 18 hours of cooling, but from then on showed lower differences than the others. After about 30 hours of cooling, the strain differences at 8 inches from the top were consistently higher than the others. After about 72 hours of cooling and continuing through the cooling period, the

cumulative strain differences at each of the three depths showed only minor variations; the maximum strain difference was 345 microstrain at the 8-inch depth. The author believes that the inherent variations of the coefficient of thermal expansion within the prism account for the variations in strain differences at 4, 8, and 12 inches from the top; calculated average coefficients of thermal expansion in 10^{6} strain per °F for the three depths are 5.4, 5.7, and 5.5, respectively, through the cooling portion of the test.

Steel strain differences, shown in Figure 11 as squares, started into the contraction or negative strain direction as expected, but after the 6-hour reading they made a reversal into the expansion or positive strain zone and remained there until the end of the test. The configuration of the welded wire fabric most likely is responsible for this anomaly. The stress (and strain) distribution in the bars, formed into a 12 by 12-inch square by welds at four points, is much different than it would be in a straight bar under the same conditions. For many years the coefficients of thermal expansion of steel and concrete have been considered to be about the same, so in the case of a plain straight steel bar in concrete, one would expect to see both steel and concrete contract about the same when cooled. With the welded wire fabric used in this study, length change of each bar segment would be resisted by the welded restraint provided by the bar at 90 degrees from it, resulting in stress distribution quite different from a straight bar.

Thermal Studies - Heating

The same prism used in the cooling tests was also used in the heating tests, in which heat was applied with infrared lamps using an on-off cycle to simulate daily exposure to a hot summer sun. Average strain and temperature differences for the heating tests are shown in Figure 12. To simulate the increasing heat of the sun, the tests started with two heat lamps for the first hour, three lamps for the next 2 hours (hottest part of the day), and finally two lamps for 2 hours to finish the heating cycle.

In Figure 12, as expected, the temperature differences closest to the top showed the most dramatic increases through the heating period, reaching a maximum of 43°F about 30 minutes into the cooling-off period, which indicates the slow rate of heat transfer downward through the concrete. Temperature differences at 8 inches and 12 inches from the top were relatively low during the heating period but continued to increase for several hours after the heating was terminated, also manifesting the slow transfer of heat downward through the concrete. Generally speaking, the cumulative temperature differences were about equal at the end of the cooling-off period.

Concrete strain differences were higher toward the top during the heating period and also exhibited the most rapid decrease in the cooling-off period. Although the concrete strain is in the same direction as the expansion strain (i.e., in the positive direction), this expansion has not been effectively resisted by the steel, since the coefficient of thermal expansion for steel and concrete are very nearly equal. For this reason, no advantage can be claimed in terms of residual strain (or stress) when the concrete is heated, such as in this test.

TABLE 9. - RESIDUAL EXPANSION STRAINS AFTER SHRINKAGE FOR 365 DAYS IN 20% RH

Depth From Top, in.	Strain[a] (microstrain) for Steel Percentages of —													Shrinkage After 365 Days in 20% RH[b]
	0.05	0.06	0.07	0.08	0.09	0.10	0.11	0.12	0.13	0.14	0.15	0.16	0.17	
0	882	857	832	807	782	757	727	697	672	642	612	582	552	238
1	835	815	790	765	740	715	690	665	640	615	590	565	535	205
2	793	768	743	723	698	673	653	628	608	588	563	543	523	182
3	753	728	703	683	663	638	618	598	578	563	543	523	508	162
4	723	698	673	653	633	613	593	578	558	543	528	513	498	147
5	692	672	647	627	607	592	572	557	542	532	517	502	492	133
6	670	645	625	605	590	575	555	545	530	520	510	500	490	120
7	652	627	612	592	577	562	547	542	527	517	507	497	487	108
8	637	617	597	582	567	552	542	532	522	512	502	492	487	98
9	617	602	582	572	557	547	537	527	517	512	502	497	487	88
10	606	591	576	566	556	541	536	526	521	511	501	496	491	79
11	595	580	570	560	555	540	535	525	520	510	500	495	495	70
12	589	579	569	559	554	544	539	529	524	514	504	499	494	61
13	582	572	567	557	552	542	542	532	527	522	512	507	502	53
14	581	571	566	561	556	551	546	536	531	526	516	511	506	44
15	574	569	569	564	559	554	549	539	534	534	524	519	514	36

[a]Residual strains were calculated by subtracting the shrinkage strains after 365 days in 20% RH, last column in the above table, from the corresponding expansion strain in Table 2; example: for p = 0.15% and 2 inches from the top, expansion from Table 2 = 745 microstrain and shrinkage strain after 365 days in 20% RH = 182 microstrain (last column above); then residual expansion strain = 745 minus 182 = 563 microstrain.

[b]Shrinkage strains (microstrain) after 365 days in 20% RH were estimated, from referenced work, to be 1.3 times the shrinkage strains at 50% RH.

TABLE 10. - RESIDUAL CONCRETE COMPRESSIVE STRESSES AFTER SHRINKAGE IN 20% RH

Depth From Top, in.	Stresses[a] (psi) for Steel Percentages of –												
	0.05	0.06	0.07	0.08	0.09	0.10	0.11	0.12	0.13	0.14	0.15	0.16	0.17
(a) For prism 12 inches thick with steel 4 inches from top													
0	5	6	7	8	9	11	13	13	16	17	18	19	21
1	6	8	10	11	12	14	15	16	17	18	20	21	22
2	8	10	11	13	13	15	16	17	18	20	21	22	24
3	10	11	13	15	15	17	18	19	20	22	22	24	24
4	10	12	14	15	17	18	19	20	21	22	23	24	25
5	12	13	15	16	17	19	20	20	22	22	23	25	25
6	12	14	16	18	17	19	21	20	22	23	23	24	25
7	12	14	15	17	18	19	20	20	21	22	23	24	25
8	12	13	15	16	17	19	19	19	20	21	23	23	23
9	12	13	15	16	16	17	19	19	20	20	21	23	24
10	12	12	14	15	15	17	17	18	19	20	21	22	22
11	10	11	12	13	14	16	16	17	17	18	19	20	20
12	8	10	11	12	12	13	13	14	15	16	17	18	18
(b) For prism 16 inches thick with steel 5 inches from top													
0	3	5	6	8	8	10	11	13	14	16	18	18	20
1	6	7	8	9	10	12	13	15	16	18	19	20	22
2	7	10	10	12	13	14	15	17	18	19	20	21	23
3	8	10	11	13	14	15	16	18	19	21	22	22	24
4	9	12	12	14	15	16	17	19	20	21	22	23	24
5	10	12	13	15	16	17	18	19	20	22	22	23	24
6	11	13	14	16	16	17	18	20	20	22	23	23	24
7	11	13	14	15	16	18	18	19	19	22	22	22	24
8	10	12	14	15	15	17	17	19	19	20	22	23	23
9	10	12	13	14	15	16	17	19	19	20	21	21	23
10	10	11	12	14	14	16	16	17	17	19	20	20	21
11	9	11	12	12	12	14	14	16	16	18	18	19	19
12	7	9	9	10	11	13	12	14	13	16	17	17	18
13	6	7	8	9	9	10	10	12	13	13	14	14	15
14	4	6	6	6	6	7	8	9	9	11	12	12	14
15	2	3	3	4	5	5	6	7	7	7	8	9	10

Depth From Top, in.	Stresses[a] (psi) for Steel Percentages of –												
	0.05	0.06	0.07	0.08	0.09	0.10	0.11	0.12	0.13	0.14	0.15	0.16	0.17
(c) For prism 20 inches thick with steel 6 inches from top													
0	3	5	5	7	8	9	11	13	14	15	17	18	20
1	5	6	7	9	10	12	13	15	15	17	19	21	22
2	7	8	9	10	12	13	15	16	17	18	20	22	23
3	7	10	11	12	13	14	16	17	18	20	21	23	24
4	8	11	11	13	14	15	17	18	19	20	21	23	24
5	8	11	12	13	15	16	18	19	19	21	21	24	24
6	10	11	13	14	15	17	18	19	20	21	22	23	24
7	9	11	12	14	15	17	18	18	18	21	21	23	24
8	9	11	12	14	14	16	17	18	19	20	21	23	22
9	9	11	12	13	14	16	17	18	18	20	20	22	23
10	9	11	11	12	13	15	16	17	16	18	19	21	21
11	7	9	10	12	12	13	14	15	15	18	18	19	19
12	6	6	9	9	10	12	12	13	13	15	17	18	18
13	5	6	7	8	9	10	10	12	12	13	14	14	15
14	3	5	6	6	7	7	8	9	9	10	11	13	14
15	2	3	3	4	4	5	6	7	7	7	8	9	10

[a]Stresses were calculated as follows: (a) For concrete stress at the steel depth, obtain the residual expansion strain after shrinkage in 20% RH from Table 9, then $f_c = \epsilon_c \times p \times E_s$; example: for p = 0.15% and steel depth of 4 inches (prism 12 inches thick), residual expansion strain after shrinkage in 20% RH = 528 microstrain (Table 9), then $f_c = (528 \times 10^{-6}) \times (0.0015) \times (29 \times 10^6) =$ 23 psi; (b) To obtain stresses for other than the steel depth: divide the residual expansion strain after shrinkage in 20% RH (Table 9) by the corresponding expansion strain in Table 2 and multiply by the corresponding expansion stress in Table 5; example: for Table 10(a) – prism 12 inches thick with steel 4 inches from the top – with p = 0.15% and depth of 1 inch from the top, residual expansion strain after shrinkage in 20% RH = 590 microstrain (Table 9), corresponding expansion strain = 795 microstrain (Table 2), corresponding expansion stress = 27 psi (Table 5a), then 590 divided by 795 x 27 = 20 psi.

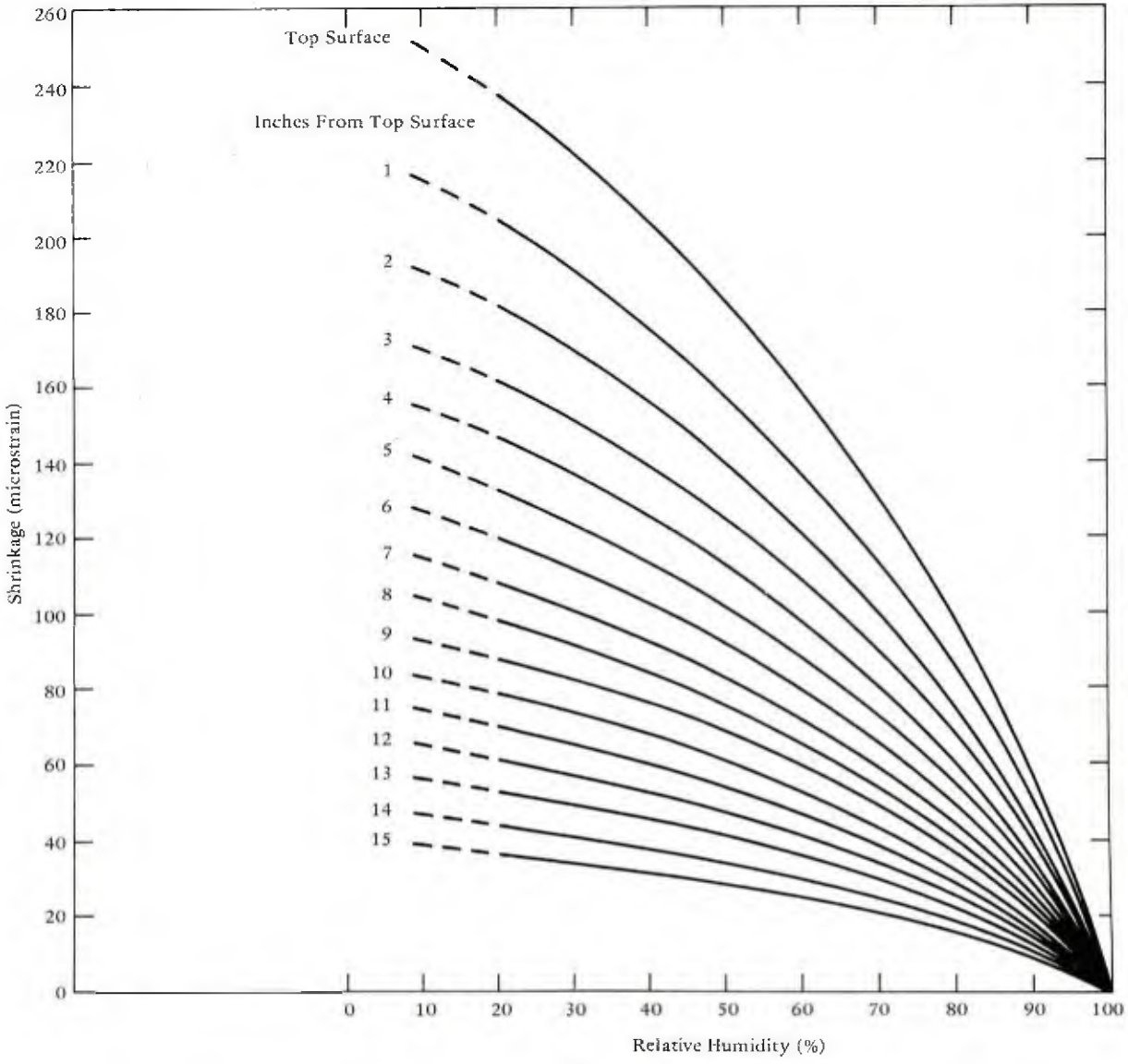

Figure 10. One-year shrinkage strains versus humidity.

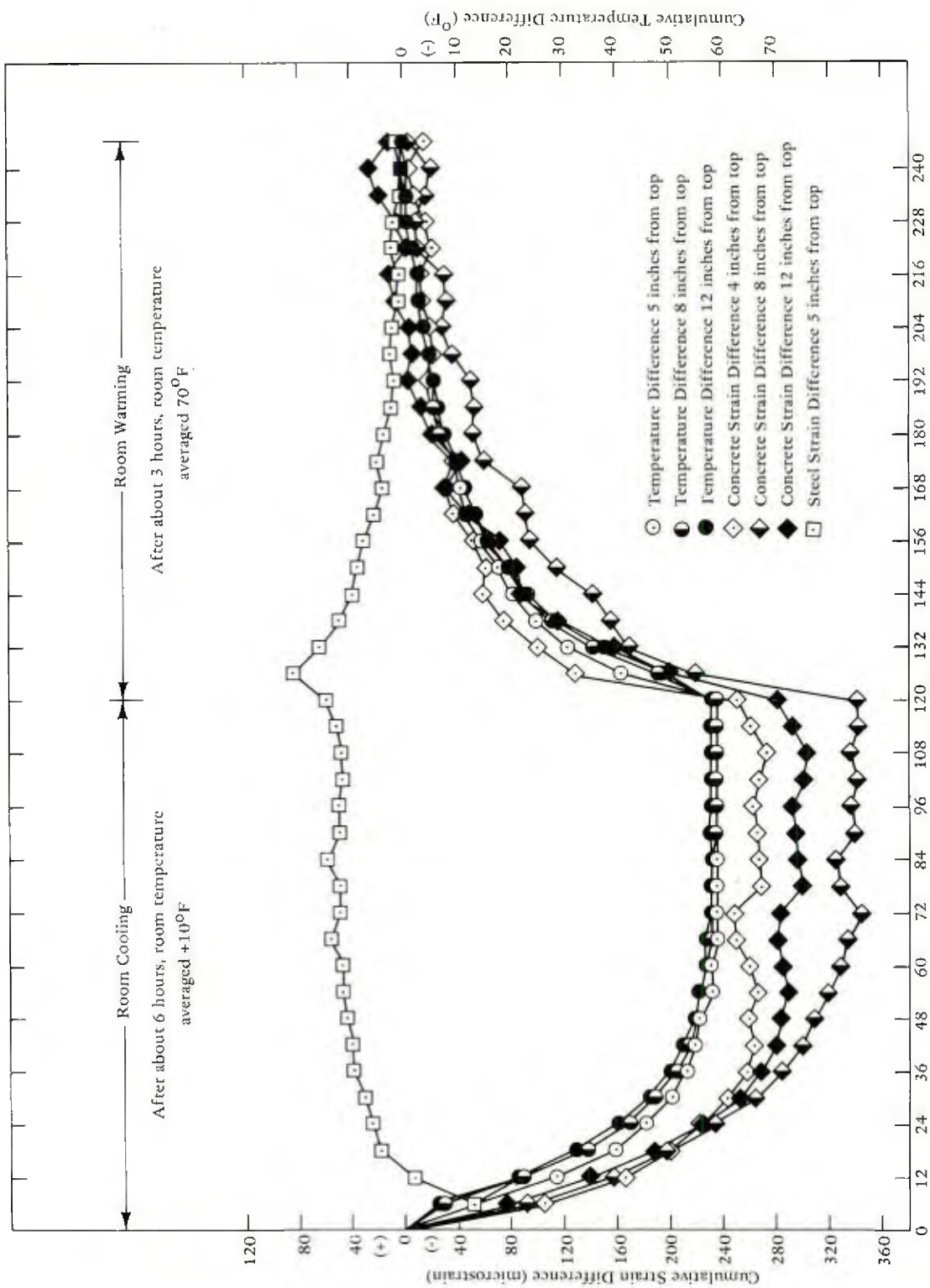

Figure 11. Results of cooling tests of prism 14 by 14 in. sq and 16 in. thick with steel percentage of 0.092%.

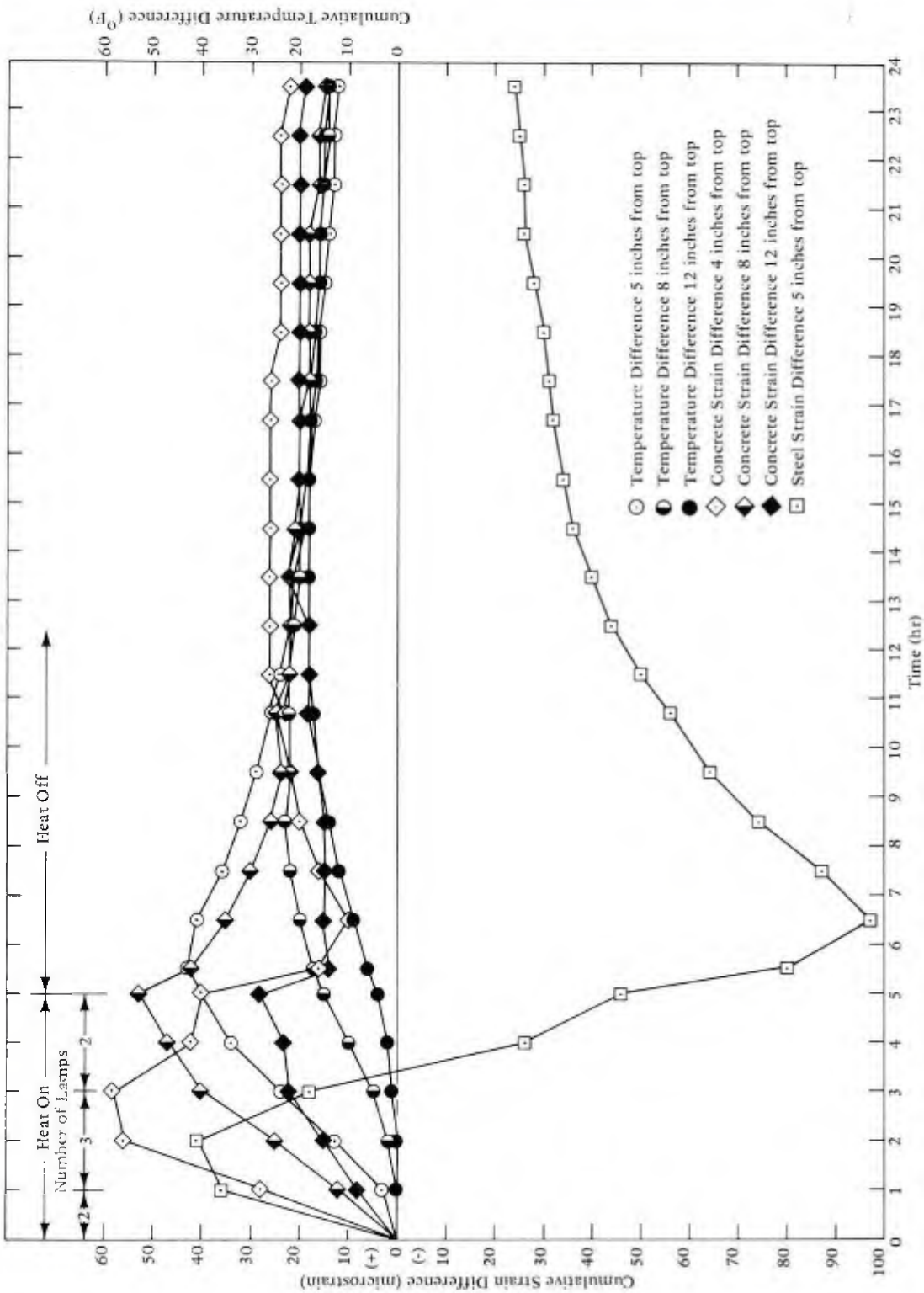

Figure 12. Results of heating tests of prism 14 by 14 in. sq and 16 in. thick with steel percentage of 0.092%.

TABLE 11. - ONE-YEAR SHRINKAGE AS A FUNCTION OF HUMIDITY

Depth From Top, in.	Shrinkage (microstrain) with Relative Humidity (%) of –									
	10[a]	20	30	40	50	60	70	75	80[a]	90[a]
0	251	238	222	203	183	159	131	115	99	58
1	216	205	192	176	158	137	113	100	86	51
2	191	182	171	157	140	121	100	88	75	45
3	170	162	151	139	125	108	89	79	67	40
4	154	147	137	126	113	97	80	71	60	35
5	141	133	124	113	102	88	73	64	55	31
6	127	120	112	103	92	80	66	58	49	28
7	114	108	101	93	83	72	59	52	44	25
8	104	98	92	84	75	65	54	47	40	22
9	93	88	83	76	68	59	49	43	36	20
10	83	79	74	68	61	53	43	38	32	17
11	74	70	65	60	54	47	39	34	29	16
12	65	61	57	52	47	41	34	30	25	14
13	56	53	50	45	41	36	29	26	22	12
14	47	44	41	38	34	30	25	22	18	10
15	39	36	34	31	28	25	21	19	16	8

[a]Shrinkage strains obtained by extrapolation.

Table 12 shows the stress differences resulting from the maximum strain changes at each of the depths during the heating tests. Stresses were calculated by dividing the strain change in Table 12, for a given depth, by the original expansion strain in Table 2 and multiplying by the concrete stress in Table 5. None of the stresses in Table 12 is significant.

Steel strain differences in Figure 12 showed an expected increase in the positive (expansion) direction for 2 hours into the heating period but thereafter exhibited a dramatic reversal into the negative or contraction zone and remained there throughout the remainder of the test.

Table 13 shows how much of the original concrete compressive expansion stresses would remain if a shrinkage-compensating airport pavement were subjected to the following conditions: (1) shrinkage at 20% RH for 1 year, and (2) sustained cold conditions as used in the cooling test, with a maximum strain contraction of 345 microstrain for the whole mass of the concrete. Stresses at the steel depth in Table 13 were obtained by subtracting the cooling contraction strain of 345 microstrain from the residual strain in Table 9 and then using the equation $f_c = \varepsilon_c \times p \times E_s$. Stresses at other depths were obtained by subtracting the cooling contraction strain of 345 microstrain from the residual strains in Table 9, dividing this difference by the corresponding original expansion strain in Table 2, and multiplying this ratio by the corresponding original expansion stress in Table 5. Results in Table 13 show that a slight concrete compressive stress remains at all depths in spite of the rather severe conditions imposed.

TABLE 12. - MAXIMUM CONCRETE STRAIN AND STRESS CHANGES DUE TO HEATING

Depth From Top, in.	Maximum Strain Change, microstrain	Maximum Stress Change[a] (psi) for Each Prism Thickness			Time After Heating Began, hr
		12 in.	16 in.	20 in.	
4	58	1.5	1.3	1.3	3
8	53	1.5	1.4	1.4	5
12	28	0.6	0.5	0.5	5

[a]With steel percentage of 0.09%, stresses were calculated by dividing the strain change in the above table by the corresponding expansion strain in Table 2 and multiplying by the corresponding expansion stress in Table 5; example: for a prism 16 inches thick at a depth of 8 inches, the strain change from above is 53 microstrain, the corresponding expansion strain from Table 2 is 665 microstrain, and the corresponding stress from Table 5(b) is 18 psi, then maximum stress change = 53 divided by 665 and multiplied by 18 = 1.4 psi.

TABLE 13. - RESIDUAL CONCRETE COMPRESSIVE STRESSES AFTER SHRINKAGE AT 20% RH AND AFTER SUBJECTION TO EXTENDED COOLING

Depth From Top, in.	Stresses[a] (psi) for Steel Percentages of –												
	0.05	0.06	0.07	0.08	0.09	0.10	0.11	0.12	0.13	0.14	0.15	0.16	0.17
(a) For prism 12 inches thick with steel 4 inches from top													
0	3	3	4	5	5	6	7	7	8	8	9	8	8
1	4	5	5	6	6	7	8	8	8	8	8	8	8
2	5	5	6	7	7	7	8	8	8	8	8	8	8
3	5	6	7	7	7	8	8	8	8	8	8	8	8
4	5	6	7	7	8	8	8	8	8	8	8	8	8
5	6	6	7	7	7	8	8	8	8	8	8	8	8
6	6	7	7	8	7	8	8	8	8	8	8	8	7
7	6	6	7	7	7	7	7	7	7	7	7	7	7
8	6	6	7	7	7	7	7	7	7	7	7	7	7
9	5	6	6	6	6	6	7	7	7	7	7	7	7
10	5	5	6	6	6	6	6	6	6	6	6	7	6
11	4	4	5	5	5	6	6	6	6	6	6	6	6
12	3	4	4	4	4	5	5	5	5	5	5	6	5
(b) For prism 16 inches thick with steel 5 inches from top													
0	2	3	4	4	5	5	6	6	7	7	8	8	8
1	3	4	4	5	5	6	7	7	7	8	8	8	8
2	4	5	6	6	6	7	7	8	8	8	8	8	8
3	4	5	6	6	7	7	7	8	8	8	8	8	8
4	5	6	6	7	7	7	7	8	8	8	8	7	7
5	5	6	6	7	7	7	7	7	7	8	7	7	7
6	5	6	6	7	7	7	7	7	7	7	7	7	7
7	5	6	6	6	6	7	6	7	7	7	7	7	7
8	5	5	6	6	6	6	6	7	7	7	7	7	7
9	5	5	5	6	6	6	6	7	6	7	7	6	7
10	4	5	5	5	5	6	6	6	6	6	6	6	6
11	4	4	5	5	5	5	5	5	5	6	6	6	6
12	3	4	4	4	4	5	4	5	5	5	5	5	5
13	3	3	3	3	3	4	4	4	4	4	5	5	5
14	2	2	2	2	2	3	3	3	3	4	4	4	4
15	1	1	1	1	2	2	2	2	3	3	3	3	3

Depth From Top, in.	Stresses[a] (psi) for Steel Percentages of –												
	0.05	0.06	0.07	0.08	0.09	0.10	0.11	0.12	0.13	0.14	0.15	0.16	0.17
(c) For prism 20 inches thick with steel 6 inches from top													
0	2	3	3	4	4	5	6	6	7	7	8	8	8
1	3	4	4	5	5	6	7	7	7	8	8	8	8
2	4	4	5	5	6	7	7	7	7	8	8	8	8
3	4	5	5	6	6	7	7	7	7	8	8	8	8
4	4	5	6	6	6	7	7	7	7	7	7	7	7
5	4	5	5	6	6	7	7	7	7	7	7	7	7
6	5	5	6	6	6	7	7	7	7	7	7	7	7
7	4	5	5	6	6	6	6	7	6	7	7	7	7
8	4	5	5	6	6	6	6	6	6	7	7	7	7
9	4	5	5	5	5	6	6	6	6	6	6	7	7
10	4	4	5	5	5	5	6	6	6	6	6	6	6
11	3	4	4	4	5	5	5	5	5	6	5	6	6
12	3	3	4	3	4	4	4	5	5	5	5	6	5
13	2	3	3	3	3	4	4	4	4	4	5	5	5
14	1	2	2	2	3	3	3	3	3	3	4	4	4
15	1	1	1	1	1	2	2	2	3	3	3	3	3

[a]Stresses were calculated as follows: (a) For concrete stresses at the steel depth, subtract the cooling contraction strain of 345 microstrain from the steel-depth residual strain in Table 9, then $f_c = \epsilon_c \times p \times E_s$; example: for Table 13(a) above – prism 12 inches thick with steel 4 inches from the top – and with p = 0.15%, residual strain in Table 9 at depth of 4 inches = 528 microstrain; 528 minus 345 = 183 microstrain; then $f_c = (183 \times 10^{-6}) \times (0.0015) \times (29 \times 10^6) = 8$ psi; (b) To obtain stresses for other than the steel depth: subtract the cooling contraction of 345 microstrain from the corresponding residual strain in Table 9, divide by the corresponding expansion strain in Table 2, and multiply by the corresponding concrete stress in Table 5; example: for Table 13(a) above, prism 12 inches thick with steel 4 inches from the top, at a depth of 1 inch from the top with p = 0.15%, residual strain in Table 9 = 590 microstrain, corresponding expansion strain in Table 2 = 795 microstrain, corresponding expansion stress in Table 5(a) = 27 psi; then 590 minus 345 = 245 divided by 795 x 27 = 8 psi.

GENERAL DISCUSSION

Design principles for rigid airport pavements are presented in Reference 2 (pp. 49-74) and Reference 11. Although design principles are based largely on analyses originated by Westergaard, choice of transverse joint spacing over the years has been influenced considerably by field experience, with due consideration to computed stresses caused by shrinkage, subgrade friction, and temperature changes (Ref 11). In addition, as Yoder and Witzak state (Ref 11), "It is evident that the stress-inducing factors are extremely complex; in some cases they cannot be evaluated except by making radically simplifying assumptions." Determination of the pavement thickness is based on the load parameters alone; joints and reinforcement take care of stresses caused by temperature changes, shrinkage, and subgrade friction (Ref 11). For slabs of average length (30 to 40 feet) warping stresses are critical, whereas for slabs 100 feet or longer, frictional resistance forces are critical (Ref 11).

Table 3-2 of Reference 2 recommends maximum transverse joint spacings of 20 feet for slabs 9 to 12 inches thick and 25 feet for slabs thicker than 12 inches. Transverse joint spacings of the Dallas-Fort Worth airport (conventional portland cement concrete) were originally 50 feet, with dowelling at each joint. When intermediate cracking was observed, joints were sawed at midlength, making the effective transverse joint spacing 25 feet. Pavement thicknesses were 15, 16, and 17 inches. The Dallas-Fort Worth design for transverse joint spacing of 50 feet rather than the recommended maximum spacing of 25 feet shows that Reference 2 is intended as a guide, and designers are given flexibility of judgment.

When considering the results of this research in terms of residual concrete compressive stresses after shrinkage, it should be observed that the conditions imposed for the data in Table 13 were assumed to be the worst. For example, shrinkage in 20% RH was taken to be the value after 1 year at a constant humidity, which is very severe since ambient humidity even in a "dry" climate varies considerably. In addition, the shrinkage strains were assumed to be completely resisted; i.e., 100% restrained shrinkage. Likewise, consideration given to stresses caused by subgrade friction when shrinkage-compensating concrete is used should take into account the "extra" induced compressive stresses in the lower portion of the slab because the subgrade resists the expansion during the curing period. Magnitude of the stresses induced by subgrade friction is unknown at this time.

To date, the most pertinent usage of shrinkage-compensating concrete in airport construction has been at Love Field in Dallas, Tex., in 1969. A mile-long taxiway 75 feet wide (in 25-foot lanes) and 14 inches thick was constructed of concrete made with Type K ChemComp in which the trans-

---

11. Yoder, E. J. and Witczak, M. W., "Principles of Pavement Design," Second Edition, John Wiley and Sons, Inc., 1975, pp. 81-125, 559-624.
12. Pinkerton, James W. and Joe V. Williams, Jr., "Expansive Cement Concrete Paving-Taxiways," Klein Symposium on Expansive Cement Concretes, SP-38, American Concrete Institute, 1973, pp. 289-297.

verse joints were 125 feet apart (Ref 12). Reinforcement was 6 x 12 welded wire fabric consisting of longitudinal 3/0 wires on 6-inch centers and transverse no. 3 wires on 12-inch centers, providing steel percentages of 0.13 longitudinal and 0.03 transverse. Only three transverse cracks have developed between the 125-foot joints in the mile-long taxiway after several years of heavy traffic. The Type K ChemComp cement used in construction of this taxiway was made by the same manufacturer who supplied the lower-expansion cement for the CEL study; as stated above, this cement provided about 62% as much 28-day expansion as the other. Thus, if a higher-expansion cement had been used in the Love Field taxiway, the joint spacing (theoretically) could have been 125/0.62 = 202 feet. The longitudinal steel percentage of 0.13 used in the Love Field taxiway was about in the middle of the steel percentage range used in this study.

The advantages of utilizing shrinkage-compensating concrete in an airport taxiway can be shown by the following example. With a 1-mile section with transverse joint spacing of 200 feet, there would be 27 joints; if spaced at 25 feet, there would be 212 joints. A considerable saving would be realized when the slab is built by not having to provide about 185 joints, not to mention maintenance of those joints over the life of the taxiway. In 1979, the incremental (premium) cost of the shrinkage-compensating (ChemComp) cement over Type I portland cement is about $5 per ton. When the above advantages are considered as well as improved "ride" for the airplanes, the extra cost seems amply justified.

CONCLUSIONS

1. Based on research data obtained in this study, expansive concrete (made with commercially available shrinkage-compensating cement) used in lightly reinforced thick slabs can induce concrete compressive stresses of sufficient magnitude to accommodate subsequent tensile stresses caused by shrinkage and heating or cooling.

2. Combining these laboratory research results with field experience at Love Field, Dallas, it is highly probable that a transverse joint spacing in excess of 125 feet is practical and feasible. A spacing of 200 feet over a length of 1 mile would mean construction and maintenance of about 27 joints instead of 212 with 25-foot spacing. The premium cost of $5 per ton for shrinkage-compensating (ChemComp) cement seems amply justified.

RECOMMENDATIONS

To study concrete expansions in a larger mass and to evaluate performance of instrumentation, it is recommended that a slab 20 feet wide, 40 feet long, and 16 inches thick be constructed at CEL with shrinkage-compensating cement having a minimum mortar bar expansion of 0.05 to 0.06 (Ref 4). The slab will be reinforced with 6 by 12-inch welded wire fabric.

For a full-sized demonstration, it is recommended that at the earliest opportunity one lane of moderate length (~1 mile) of a taxiway construction section be designated as a research project. This section is to be made with shrinkage-compensating cement having a minimum mortar bar expansion of 0.05 to 0.06; all other parameters would be the same as specified for the rest of the project (thickness, steel percentage, placement, etc.). It is also highly recommended that provision be made for strain gage and length change instrumentation of the shrinkage-compensating concrete slab so that full-scale field data can be obtained both during the expansion or curing period and after the slab has gone into service. It is further recommended that transverse joint spacing in this 1-mile section be a nominal 200 feet. A suggested joint spacing might be as follows: the first 10 joints at 200 feet, the next 5 joints at 175 feet, the next 5 joints at 225 feet, and the remaining 6 joints at 200 feet. Such an installation would establish field data on which to base subsequent full-scale designs for shrinkage-compensating airport slabs with substantially fewer transverse joints, lower joint maintenance costs, and much smoother running surfaces for aircraft.

ACKNOWLEDGMENTS

The author gratefully acknowledges the assistance and cooperation of the following companies and their representatives in supplying cement and aggregates in a time of shortages:

Southwestern Portland Cement Company - Mr. Taylor Test

Texas Industries - Mr. Joe Williams

Chemically Prestressed Concrete Corporation - Mr. Bill Liljestrom

The author also appreciates the many constructive comments on the draft of this report by Mr. H. Tomita (FAA), Dr. W. S. Haynes, Mr. E. J. Barenberg, Dr. James Forrest, and Mr. Robert J. Gulyas, in addition to those named above. The author recognizes that the success of a research study of this magnitude depends upon consistent day-by-day performance by dependable technicians. The author wishes to thank Mr. J. A. Crahan, Mr. J. D. Gurrola, and Mr. V. Hernandez, who also coordinated all research tests.

REFERENCES

1. J. R. Keeton, "Shrinkage-Compensating Cement for Airport Pavement," Federal Aviation Administration Report No. FAA-RD-75-89, June 1975.

2. Federal Aviation Administration, Advisory Circular 150/5320-6B, Airport Pavement Design and Evaluation, May 28, 1974, pp. 73, 74.

3. Federal Aviation Administration, Advisory Circular 150/5370-10, Standards for Specifying Construction of Airports, October 24, 1974, pp. 332, 319, 320.

4. American Society for Testing and Materials, Standard Method for Restrained Expansion of Expansive Cement Mortar, ASTM C806-75, Vol. 13, 1978, pp. 468-472.

5. _____. Standard Test Method for Restrained Expansion of Shrinkage-Compensating Concrete, ASTM C878-78, Vol. 14, 1978, pp. 547-550.

6. American Concrete Institute. Recommended Practice for the Use of Shrinkage-Compensating Concrete, ACI Standard 223-77, 1977.

7. Naval Civil Engineering Laboratory. Technical Report R-333-I, Study of Creep in Concrete--Phase I, by John R. Keeton, Port Hueneme, California, January 1965.

8. _____. Technical Report R-333-III, Study of Creep in Concrete--Phases 3, 4, and 5, by John R. Keeton, Port Hueneme, California, May 1965.

9. _____. Technical Report R-704, Creep and Shrinkage of Reinforced Thin-Shell Concrete, by John R. Keeton, Port Hueneme, California, November 1970.

10. Civil Engineering Laboratory. Technical Note N-1504, Expansive Cement Concretes for Naval Construction, by John R. Keeton, Port Hueneme, California, November 1977.

11. E. J. Yoder and M. W. Witczak, "Principles of Pavement Design," Second Edition, John Wiley and Sons, Inc., 1975, pp. 81-125, 559-624.

12. James W. Pinkerton and Joe V. Williams, Jr., "Expansive Cement Concrete Paving--Taxiways," Klein Symposium on Expansive Cement Concretes, SP-38, American Concrete Institute, 1973, pp. 289-297.

Appendix A

PHASE 3: SHRINKAGE-COMPENSATING CEMENT IN FIBROUS CONCRETES

Phase 3 involves an investigation of the practicability of using shrinkage-compensating cement in fibrous concrete for overlays of airport pavements.

EXPERIMENTAL PROGRAM

To provide some research data on which to base a decision to proceed with a full-scale research study (Phase 4), the following parameters were used.

Water-cement ratio	.0.5
Cement plus fly ash	.7.9, 9.3, and 10.7 bags/cu yd
Fiber content	.1-1/2% by volume of mix
River aggregate	.3/8-inch maximum size
Specimen size in plan	.12 by 12 inches
Specimen thickness	.6 inches
Number of specimens	.One for each variable (6 total)
Shrinkage environments	.50% and 75% RH

Strength tests were made with the same mix using Type II portland cement for comparison. Curing for 28 days was done in the same manner as before (the top covered with wet burlap, sealed with aluminum foil, sides coated with butyl).

PRELIMINARY TEST RESULTS

Preliminary test results are shown in Figure A-1 for two prisms 6 inches thick made with cement plus fly ash contents of 7.9 and 10.7 bags/cu yd. At 1 year of age both prisms showed sizeable amounts of expansion strain remaining. Calculation of corresponding concrete stresses must await determination of the equivalent steel percentages which the various fiber contents represent. Based on results presented in Figure A-1, use of shrinkage-compensating fibrous concrete for construction of airport pavement overlays shows definite promise.

Figure A-2 compares flexural strengths of fibrous concretes made with portland Type II and with shrinkage-compensating cements. Shrinkage-compensating fibrous concrete provides slightly higher flexural strength.

RECOMMENDATIONS

To experimentally determine the optimum combinations of cement content and fiber content for fibrous shrinkage-compensating concretes to be used in airport overlays, the following are recommended for the research program.

Fiber contents	1%, 1-1/2%, 2% (aspect ratio = 100)
Cement content	6.0, 8.0, 10.0 bags/cu yd
Specimen thickness	4, 6, 8 inches
Shrinkage environment	50, 75% RH
Total number of specimens	162

Research data obtained in this research program will provide a basis for technical specifications for fibrous concrete overlays of shrinkage-compensating concretes with fewer transverse joints.

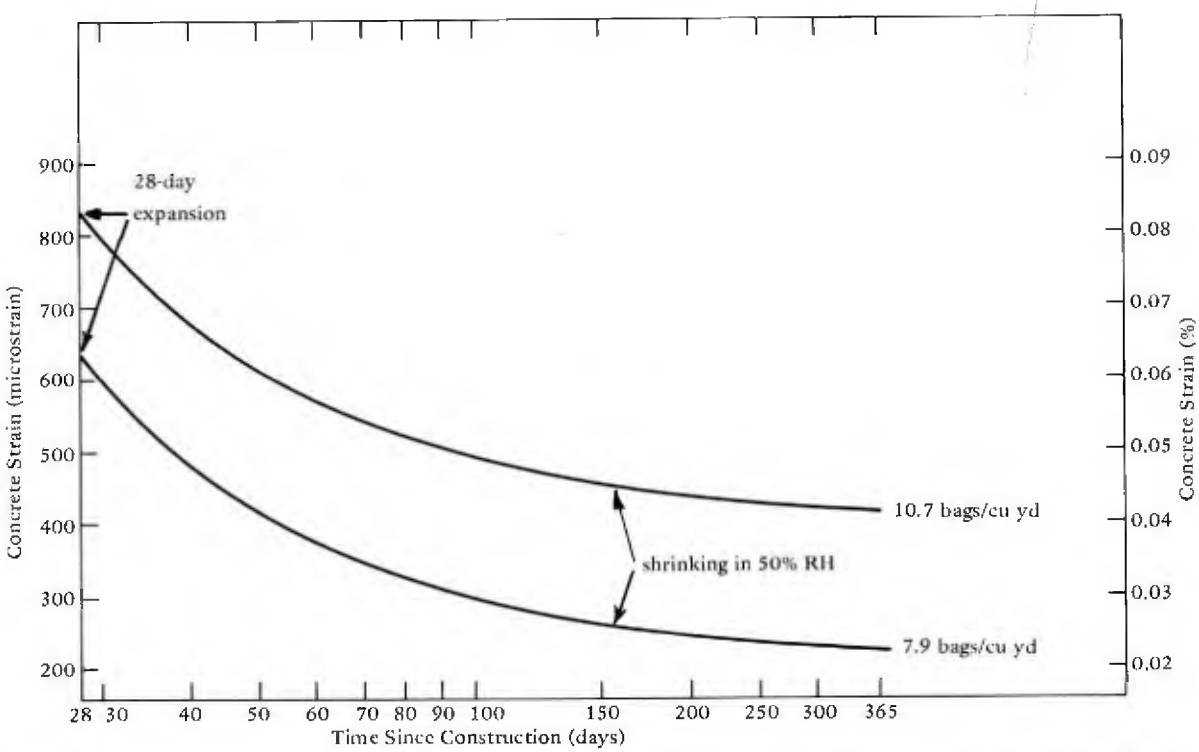

Figure A-1. Preliminary expansion-shrinkage data for two 1-ft sq prisms 6 in. thick with 1-1/2% steel fibers and 1 in. long of shrinkage-compensating fibrous concrete.

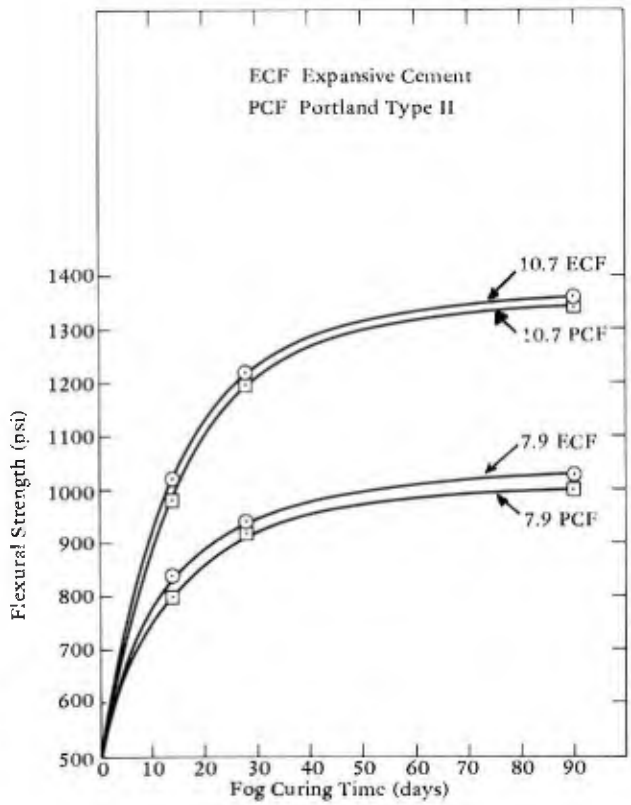

Figure A-2. Flexural strengths of fibrous concretes with 7.9 and 10.7 bags of cement per cubic yard.

Appendix B

STEEL EXPANSION STRAINS

Steel expansion strains are presented in Figure B-1 for the steel percentages used in this study. A least-squares line is shown, although the data are somewhat erratic. The author believes that the welding of the bars into fairly rigid rectangular shapes drastically affects the strain (and stress) distribution and makes correlation with concrete strains extremely difficult, if not impossible. Since concrete strains are of primary importance in this study, the steel strains were not included in the main body of this report.

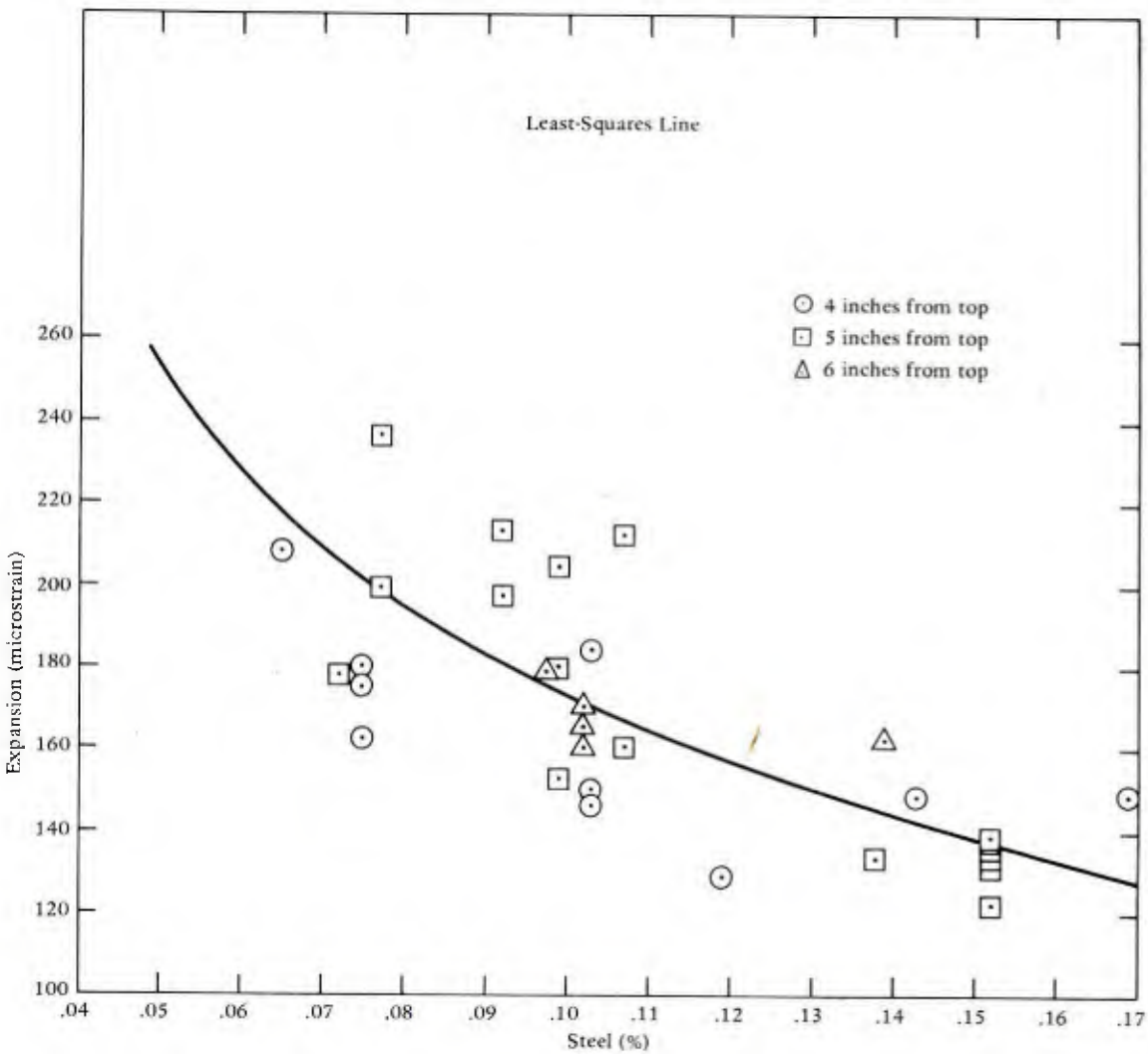

Figure B-1. Steel expansion strains after 28 days of curing.

DISTRIBUTION LIST

AAP NAVORDSTA IND HD DET PWO (Code 092) McAlester OK
AF AERO DEF COM HQS/DEE (T. Hein), Colorado Springs CO
AF HQ PREEU, Washington DC
AFB (AFIT/LD), Wright-Patterson OH; AF Tech Office (Mgt & Ops), Tyndall, FL; AFCEC/DE Tyndall, FL; AFETO/DOSE, Tyndall AFB, FL; AFIT DET (Meyer) Wright-Patterson, OH; Air Base Group (MAC), Attus AFB, OK; CESCH, Wright-Patterson; DET Wright-Patterson OH; HQ Tactical Air Cmd (R. E. Fisher), Langley AFB VA; HQAFESC/DEMM, Tyndall AFB, FL; HQSAC DEPM, Offutt, NE; MAC/DET (Col. P. Thompson) Scott, IL; Stinfo Library, Offutt NE
AFWL CE Div., Kirtland AFB NM
AFB (LT Acero), McGuire AFB, NJ
ARMY BMDSC-RE (H. McClellan) Huntsville AL; CFLD Engr (MAJ R. Shurb), Fort Belvoir VA; DAEN-MPE-D Washington DC; HQ-DAEN-MPO-B (Mr. Price); HQDA (DAEN-FEE-A)
ARMY - CERL Library, Champaign IL
ARMY COE Philadelphia Dist. (LIBRARY) Philadelphia, PA
ARMY CORPS OF ENGINEERS MRD-Eng. Div., Omaha NE; Seattle Dist. Library, Seattle WA
ARMY CRREL R.A. Eaton
ARMY DARCOM AMCPM-CS (J. Carr), Alexandria VA; Code DRCPM-CS, Alexandria VA
ARMY ENG WATERWAYS EXP STA Director Vicksburg, MS; Library, Vicksburg MS
ARMY ENVIRON. HYGIENE AGCY Water Qual Div Doner), Aberdeen Prov Ground, MD
ARMY MATERIALS & MECHANICS RESEARCH CENTER Dr. Lenoe, Watertown MA
ARMY MOBIL EQUIP R&D COM Tech. Library (Vault) Fort Belvoir VA
ARMY TRANSPORTATION SCHOOL ATSP-CTD-MS Fort Eustis, VA; MAJ T Sweeney, Code ATSP CD-TE Fort Eustis VA
ASO PWO, Philadelphia PA
ASST SECRETARY OF THE NAVY Dir. of Instal/Facil. Washington DC; R&D Washington, DC; Spec. Assist Energy (Leonard), Washington, DC
ATOMIC ENERGY COMMISSION Knolls Lab (Library)I dhenectady, NY
CHNAVPERS Code PERS-M113, Washington DC; Code PERS-M12 Wash, DC; Naval Milpers Cmd (NMPC 643), Wash., D.C.
CINCLANT Civil Engr. Supp. Plans, Ofr Norfolk, VA
CINCPAC Fac Engrng Div (J44) Makalapa, HI
CINCPAC LT SCE, Pearl Harbor HI
CNM NMAT - 08T242 Washington, DC; NMAT 08T4 (P.B. Newton), Washington DC
CNO Code NOP-964, Washington DC
COMCBPAC Operations Off, Makalapa HI
COMFAIRJAX Security Offr, Jacksonville FL
COMFAIRMED Security Offr, Naples, Italy
COMFAIRWESTPAC Security Offr, Misawa Japan
COMFAIRWESTPAC DET MISAWA PWO, Misawa, Japan
COMFLEACT, OKINAWA SCE, Yokosuka Japan
COMFLTAIR West Pac Staff Civil Engineer Atsugi Japan
COMNAVAIRPAC Code 53, San Diego, CA
COMNAVBEACHPHIBREFTRAGRU ONE San Diego CA
COMNAVDIST PWD Code 412, Washington DC
COMNAVLOGPAC SCE, Pearl Harbor HI
COMNAVMARIANAS Code N4, Guam; FLTWEATHCENSUPOFFR, Guam
COMNAVSUPPFORANTARCTICA PWO
COMOCEANSYSPAC SCE, Pearl Harbor HI
COMSUBDEVGRUONE Operations Offr, San Diego, CA
DEFENSE DOCUMENTATION CTR Alexandria, VA
DEFENSE ELEC SUP CEN PWO, Dayton OH
DIR. DEFENSE RSCH & ENGR Pentagon (Rm 3C-128), Washington DC
DLSIE Army Logistics Mgt Center, Fort Lee, VA
DNA STTL, Washington DC; Tech. Services Library, Mercury NV
DNL Washington DC

DTNSRDC Code 4120 (Hall), Annapolis MD
DTNSRDC PWO
FLDSUPPACT SCE, Washington DC
FLTCOMBATRACENLANT Code 182, Virginia Bch VA
FMFLANT CEC Offr, Norfolk VA
FMFPAC (CDR Shank), Pearl Harbor HI
FOREST SERVICE Engr Staff (Colley), Wash, D.C.
GSA Ch. Spec. Div./Pub. Bldg Serv., POX, Washington DC
IBERLANTAREA Code C-4, Lisbon PO
MARCORPS AIR/GND COMBAT CTR LT M. Perry, Twentynine Palms CA; PWO, Twentynine Palms CA
MARINE CORPS AIR STA PWO Beaufort SC
MARINE CORPS BASE Code 43-260, Camp Lejeune NC; Commander, Pacific, Pearl Harbor HI; M & R Division, Camp Lejeune NC; PWO Camp Lejeune NC; PWO, Camp Pendleton CA; PWO, Camp S. D. Butler, Kawasaki Japan
MARINE CORPS HQS Code LFF-2, Washington DC
MARINE CORPS LOGISTICS SUPPORT ACT. PWO, Albany GA
MARITIME ADMIN (Poretz), Washington, DC
MCAS Code 44, Cherry Point NC; Facil, Engr. Div. Cherry Point NC; PW0, Beaufor SC; (Bergstrom), Code IJF, El Toro, Santa Ana, CA; Code PWE, Kaneohe Bay HI; Code S4, Quantico VA; PW Inspection BrSnch, El Toro, Santa Ana CA; PWO - Santa Ana, CA; PWO Kaneohe Bay HI; PWO, Iwakuni Japan; PWO, Kaneohe, HI; PWO, Yuma AZ; SCE, Futema Japan
MCDEC Base Maint. Ofr. Quantico, VA; M & L Div Quantico, VA; NSAP REP. Quantico VA; P&S Div Quantico VA
MCLSBPAC PWO, Barstow CA
NAD PWO Hawthorne, NV
NAF PWD - Engr Div, Atsugi, Japan; PWO Sigonella Sicily; PWO, Atsugi Japan; PWO, Mount Clemens MI
NARF Code 640, Pensacola FL
NAS CO, Code 70; CO, Guantanamo Bay Cuba; Code 114, Alameda CA; Code 1821 H, Miramar, San Diego CA; Code 183 (Fac. Plan BR MGR); Code 18300, Lemoore CA 93245; Code 1832, Jacksonville FL; Code 183P (J. Howald), Corpus Christi TX; Code 18700, Brunswick ME; Code 18A, Miramar, San Diego CA; Code 18U (ENS P.J. Hickey), Corpus Christi TX; Code 70, Atlanta, Marietta GA; Dir. Maint. Control Div., Key West FL; e ir. Util. Div., Bermuda; ENS Buchholz, Pensacola, FL; ENS C. Winsor, Moffett Field CA; ENS J. Shrewsbury Point Mugu, CA; ENS L. Bochet, Kingsville TX; ENS W. Paine, Glenview IL; Engr Div Dir, Meridian MS; Guantanamo Bay Cuba; Lakehurst, NJ; OIC CBU-402, Pensacola FL; PW (J. Maguire), Corpus Christi TX; PW Maintenance Control Div. 72, Dallas TX; PWD (ENS Foshee), Chase Field, Beeville TX; PWD Maint. Cont. Dir., Fallon NV; PWD Maint. Div., New Orleans, Belle Chasse LA; PWD, Maintenance Control Dir., Bermuda; PWD, Willow Grove PA; PWO (Code 18.2), Bermuda; PWO Belle Chasse, LA; PWO Chase Field Beeville, TX; PWO Jacksonville, FL; PWO Key West FL; PWO Meridian, MS; PWO NI, San Diego Ca; PWO Patuxent River MD; PWO Point Mugu, CA; PWO Whidbey Is, Oak Harbor WA; PWO Whiting Fld, Milton FL; PWO, Aux Fallon, NV; PWO, Cecil Field FL; PWO, Corpus Christi TX; PWO, Cubi Point, R.P.; PWO, Dallas TX; PWO, Glenview IL; PWO, Kingsville TX; PWO, Lakehurst NJ; PWO, Lemoore, CA; PWO, Millington TN; PWO, Miramar, San Diego CA; PWO, Oceana, Virginia Bch VA; PWO, So. Weymouth MA; PWO,, Moffett Field CA; ROICC Key West FL; SCE Air Rework Fac. Norfolk, VA; SCE Lant Fleet Norfolk, VA; SCE Norfolk, VA; SCE Pensacola, FL; SCE, Agana Guam; SCE, Alameda CA; SCE, Barbers Point HI; SCE, Guantanamo Bay Cuba; Security Offr, Alameda CA; Shore Facil. Ofr Norfolk, VA
NATL RESEARCH COUNCIL Naval Studies Board, Washington DC
NATPARACHUTETESTRAN PW Engr, El Centro CA; PWO, ENS T.F. Dreyer, El Centro CA
NAVACT PWO, London UK
NAVAEROSPREGMEDCEN Pub Wks Dept (Dillinger) Pensacola, FL; SCE, Pensacola FL
NAVAIRDEVCEN OIC/ROICC, Warminster PA; PWO Warminster, PA
NAVAIRSYSCOM Code NAIR 4012, Washington DC
NAVAIRTESTCEN PATUXENT RIVER PWD (F. McGrath), Patuxent Riv.,MD
NAVAL RES OFFICERS TRNG CORPS UNIT (Corrigan) Purdue Univ
NAVCHAPGRU Engr. Dept. (Beckman) Williamsburg, VA
NAVCOASTSYSCEN Code 772 (C B Koesy) Panama City FL
NAVCOASTSYSTCTR Code 713 (J. Quirk) Panama City, FL; Library Panama City, FL; PWO Panama City, FL
NAVCOMMAREAMSTRSTA PWO, Norfolk VA; PWO, Wahiawa HI; SCE Unit 1 Naples Italy; Security Offr, Hawaii
NAVCOMMSTA Code 401 Nea Makri, Greece; Library, Diego Garcia Island; Maintenance Code 63 Ponce P.R.; OICC, Nea Makri Greece; PWO Nea Makri, Greece; PWO, Exmouth, Australia

NAVCOMMU PW Dept, Thurso, Scotland
NAVCONSTRACEN CO, Port Hueneme CA; Co, Gulfport MS
NAVDET PWO, Souda Bay Crete
NAVEDTRAPRODEVCEN SCE, Pensacola FL; Tech. Library
NAVEDUTRACEN Engr Dept (Code 42) Newport, RI; PWO Newport RI
NAVELEXSYSCOM ELEX-01F; PME 124-612, Wash DC
NAVFAC PWO Pacific Beach WA; PWO, Antigua; PWO, Centerville Bch, Ferndale CA
NAVFAC PWO, Lewes DE
NAVFAC PWO, Turks Is West Indies
NAVFACENGCOM Code 03 Alexandria VA; Code 03 Alexandria, VA; Code 031 Alexandria VA; Code 032A Alexandria VA; Code 032B Alexandria VA; Code 04 Alexandria VA; Code 041 Alexandria, VA; Code 043 Alexandria, VA; Code 044 Alexandria, VA; Code 0451 (P.W. Brewer) Alexandria, VA 22332; Code 0451 Alexandria, VA; Code 0451C (M.P. Jones) Alexandria, VA; Code 0454B Alexandria, Va; Code 04B1 (P.P. Brown) Alexandria VA; Code 04B5 Alexandria, VA; Code 10 Alexandria VA; Code 100 Alexandria, VA; Code 1002B (J. Leimanis) Alexandria, VA; Code 1013 Alexandria, VA; Code 1113 (T. Stevens) Alexandria, VA; Morrison Yap, Caroline Is.; OICC Field Office Ponape, ECI; OICC Field Office Ponape, ECI; P W Brewer Alexandria, VA; ROICC Code 495 Portsmouth VA
NAVFACENGCOM - CHES DIV. CO, Washington DC; Code 101 Wash, DC; Code 102, (Wildman), Wash, DC; Code 405 Wash, DC
NAVFACENGCOM - LANT DIV. Code 405 Civil Engr BR Norfolk VA; Code 405, Norfolk, VA; Code 411 Soil Mech & Paving BR Norfolk VA; Engr Adv Lat Amer, CZ; Eur. BR Deputy Dir, Naples Italy; European Branch, New York; RDT&ELO 102, Norfolk VA
NAVFACENGCOM - NORTH DIV. Asst. Dir., Great Lakes IL; CO; CO, Brooklyn NY; Code 09P (LCDR A.J. Stewart); Code 102; Code 1028, RDT&ELO, Philadelphia PA; Code 405 Civil Engr BR Philadelphia, PA; Code 111 WFT (Tayler), Phila PA
NAVFACENGCOM - PAC DIV. (Kyi) Code 101, Pearl Harbor, HI; Code 2011 Pearl Harbor, HI; Code 402, RDT&E, Pearl Harbor HI; Code 405 Civil Engr BR Pearl Harbor HI; Code 406 Spec/Cost Engrg B ‹Pearl Harbor HI; Commander, Pearl Harbor, HI
NAVFACENGCOM - SOUTH DIV. CO, Charleston SC; Code 102 Soil Mech & Paving BR Charleston, SC; Code 405 Civil Engr BR Charleston SC; Code 405, RDT&ELO, Charleston, SC; Code 411 Soil Mech & Paving BR Charleston, SC; Code 90, RDT&ELO, Charleston SC
NAVFACENGCOM - WEST DIV. 102; Code 04B San Bruno, CA; Code 401 (Bertrand) San Bruno, CA; Code 405 Civil Engr BR San Bruno CA; Code 411 Soil Mech & Paving BR San Bruno CA; O9P/20 San Bruno, CA; RDT&ELO Code 2011 San Bruno, CA; Seattle Br. Dir., Seattle WA
NAVFACENGCOM CONTRACT AROICC, Code 1042.2, Vallejo CA; AROICC, Point Mugu CA; Bethesda, OICC, Alexandria VA; Dep. OICC, Code 04 TRIDENT, Bremerton WA; ENS J. Bank, Guam; Eng Div dir, Southwest Pac, Manila, PI; OICC Mid Pacific, Pearl Harbor HI; OICC Trident, Alexandria VA; OICC, Guam; OICC, Madrid, Spain; OICC, Southwest Pac, Manila, PI; OICC/ROICC, Balboa Canal Zone; R40 AROICC Puget Sound Shpyd; ROICC AF Guam; ROICC LANT DIN., Norfolk VA; ROICC Off Point Mugu, CA; ROICC, Keflavik, Iceland; ROICC-OICC-SPA, Norfolk, VA
NAVHOSP LT R. Elsbernd, Puerto Rico; PWO, Beaufort SC
NAVINACTSHIPSTORFAC PWO, Orange TX
NAVMAG SCE, Subic Bay, R.P.; Security Offr, Hawaii
NAVMEDRSCHU 3 PWO, Cairo U.A.R
NAVOBSY PWO, Washington DC
NAVOCEANSYSCEN Code 523 (Hurley), San Diego, CA
NAVORDMISTESTFAC PWO, White Sands Missile Range NM
NAVORDSTA MDS-25, Mfg Tech Dept Louisville, KY; PWO, Indianhead, MD
NAVPETOFF Code 30, Alexandria VA
NAVPGSCOL Code 69 (T. Sarpkaya), Monterey CA
NAVPHIBASE CO, ACB 2 Norfolk, VA; Code S3T, Norfolk VA; Code S3T, Norfolk VA; PWO Norfolk, VA; SCE, Coronado, San Diego CA
NAVRADSTA PWO Jim Creek, Oso WA
NAVREGMEDCEN Gen. Engr-Maint. Control, Portsmouth VA; PWO, Camp Lejeune NC; SCE (D. Kaye); SCE, Camp Pendleton CA
NAVREGMEDCEN SCE, Great Lakes IL
NAVREGMEDCEN SCE, Long Beach CA; SCE, Oakland CA; SCE, Philadelphia PA
NAVSAFECEN NAS, Norfolk, VA

NAVSCOLCECOFF C20M (H. Welsh) Pot Hueneme, CA; C35 Port Hueneme, CA
NAVSCSOL PWO, Athens GA
NAVSEASYSCOM Code 0325, Program Mgr, Washington, DC; Code 03314, Wash. D C; Code 0701 Washington, DC; Code SEA 047 Washington, DC; Code SEA 70-C Washington, DC
NAVSECGRUACT PWO Winter Harbor ME; PWO, Adak AK; PWO, Skaggs Is, Sonoma CA
NAVSECGRUCOM Code G43, Washington DC
NAVSECSTA PWO, Washington DC
NAVSHIPYD Code 202.3, Charleston SC; Code 404 (LT J. Riccio), Norfolk, Portsmouth VA; Code 410, Mare Is., Vallejo CA; Code 440 Portsmouth NH; Code 440 Portsmouth, NH; Code 440, Puget Sound, Bremerton WA; Code 440.1 (D. Powell) Long Beach, CA; Code 444, Philadelphia PA; LTJG R. Lloyd, Vallejo CA; PW Dept (Brockwell), Charleston, SC; PWO Charleston Naval Shipyard, Charleston SC; PWO Long Beach; PWO, Norfolk; Pub Wks Dept (Wells) Long Beach, CA; Tech Library, Vallejo, CA; Utilities & Energy Cons. Mgr Code 108.1, Pearl Harbor, HI
NAVSTA Adak, AK; CO Roosevelt Roads P.R. Puerto Rico; Code 16P, Keflavik, Iceland; Maint. Control Div., Adak; Maint. Div. Dir/Code 531, Rodman Canal Zone; Maintenance Div., Rota, Spain; PWD (LTJG.P.M. Motolenich), Puerto Rico; PWO, Argentia Newfoundland; PWO, Guantanamo Bay Cuba; PWO, Keflavik Iceland; PWO, Mayport FL; SCE, San Diego CA; SCE, Subic Bay, R.P.
NAVSUBASE PWO
NAVSUPPACT LTJG McGarrah, SEC, Vallejo, CA; PWO Naples Italy; PWO, Brooklyn NY; PWO, New Orleans LA; SCE, Long Beach CA; SCE, Mare Is., Vallejo CA
NAVSUPPFAC PWO, Thurmont MD
NAVSURFLANT N10 - Base Mgmt, Norfolk VA
NAVSURFWPNCEN PWO, White Oak, Silver Spring, MD
NAVTECHTRACEN SCE, Orlando FL; SCE, Pensacola FL
NAVTELCOMMCOM Washington DC
NAVUSEAWARENGSTA Engr. Div. (Code 083) Keyport, WA; PWO, Keyport WA
NAVWARCOL Dir. of Facil., Newport RI
NAVWPNCEN Code 2636 (W. Bonner), China Lake CA; ROICC, Code 7002, China Lake CA
NAVWPNSTA PW Office (Code 09C1) Yorktown, VA
NAVWPNSTA PWO Colts Neck, NJ; PWO, Seal Beach CA
NAVWPNSTA-ST JULIENS ANNEX Asst PWO,, Portsmouth, VA
NAVWPNSUPPCEN Code 09 Crane IN; ENS J. Wyman, Crane IN
NCBU 405 OIC, San Diego, CA
NSC SCE, Charleston, SC
PWC Code 420, Pensacola, FL
NCBC CEL AOIC Port Hueneme CA; CO Davisville, RI; CO, Gulfport MS; Code 10 Davisville, RI; Code 15, Port Hueneme CA; Code 155, Port Hueneme CA; Code 156, Port Hueneme, CA; Code 400, Gulfport MS; PWO (Code 82), Port Hueneme CA; PWO Gulfport, MS; PWO, Davisville RI; Port Hueneme CA
NCBU 416 OIC, Alameda CA
NCR 20, Code R31 Gulfport, MS; 20, Code R70; 20, Commander; 30, Guam, Commander; 31, Port Hueneme, Chief of Staff
NMCB 1, CO; 1, Code S3E; 133, CO; 3, CO; 4, CO; 5, CO; 5, Operations Dept.; 62, CO; 4, CO; 74, ENS Vesely; FIVE, Operations Dept; Forty, CO; THREE, Operations Off.
NORDA Code 213 (Pyle), Bay St. Louis, MS; Code 440 (Ocean Rsch Off) Bay St. Louis MS
NRL PWO, Washington DC
NSC SCE (Code 70), Oakland CA; SCE Norfolk, VA
NSD SCE, Subic Bay, R.P.
NTC OICC, CBU-401, Great Lakes IL; PWO (Code 523) Orlando, FL; SCE, San Diego CA
NUSC Code 131 New London, CT; Code 4123 New London, CT; Code EA123 (R.S. Munn), New London CT; PWO AUTEC West Palm Bch Det. West Palm Beach, FL; PWO New London, CT; PWO Newport, RI; SB322 (Tucker), Newport RI; SCE AUTEC Andros Ranges Det.
OFFICE SECRETARY OF DEFENSE DASD (I&H) IC Pentagon (LCDR Morrison)
ONR Code 700F Arlington VA; DrNA. Laufer, Pasadena CA; LCDR Williams, Boston, MA; Nelson, Arlington, VA
PACMISRANFAC CO, Kekaha HI; PWO, Hawaiian Area, Barking Sands, Kekaha HI
PHIBCB 1 P&E, Coronado, CA; 1, CO San Diego, CA
PMTC Pat. Counsel, Point Mugu CA

PWC CO Norfolk, VA; CO Yokosuka, Japan; CO, (Code 10), Oakland, CA; CO, Great Lakes IL; CO, Guam; CO, Pearl Harbor HI; CO, San Diego CA; CO, Subic Bay, R.P.; Code 10, Great Lakes, IL; Code 100, Great Lakes, IL; Code 101, San Diego, CA; Code 105, Oakland, CA; Code 120, Oakland CA; Code 120, San Diego CA; Code 120C, (Library) San Diego, CA; Code 128, Guam; Code 154, Great Lakes, IL; Code 200 (H. Koubenec), Great Lakes IL; Code 200, Guam; Code 200, Subic Bay, R. P.; Code 220 Oakland, CA; Code 220.1, Norfolk VA; Code 240, Subic Bay, R.P.; Code 241, Subic Bay, RP; Code 30C, San Diego, CA; Code 400, Great Lakes, IL; Code 400, Oakland, CA; Code 400, Pearl Harbor, HI; Code 400, San Diego, CA; Code 420, Great Lakes, IL; Code 420, Oakland, CA; Code 420, San Diego, CA; Code 500 (R. Smith) Norfolk, VA; Code 500, Great Lakes, IL; Code 500, Oakland, CA; Code 500, San Diego, CA; Code 600, Great Lakes, IL; Code 610, San Diego Ca; Code 700, Great Lakes, IL; Code 800, San Diego, CA; ENS J.C. Yeakley, Yokosuka Japan; Library, Subic Bay, R.P.; Maint. Control Dept (R. Fujii) Pearl Harbor, HI; Planning Officer, Norfolk, VA; Pub Wks Dept (Shepard), Pearl Harbor, HI; Utilities Officer, Guam; XO (Code 20) Oakland, CA
SUPANX PWO, Williamsburg VA
U.S. MEo CHANT MARINE ACADEMY Kings Point, NY (Reprint Custodian)
US FORCES, JAPAN Nakahara Honshu; Petroleum Staff Officer Yokota AB
US NAVAL FORCES Korea (ENJ-P&O)
USAFE Dee (Hart-CAPT USAF)
USCG G-EOE-4/61 (T. Dowd), Washington DC
USCG ACADEMY PWO New London, CT; Utilities Section New London, CT
USDA Forest Service Region 3, Albuquerque, NM; Forest Service, Bowers, Atlanta, GA; Forest Service, Region 1, Missoula, MT; Forest Service, Region 4, Ogden, UT; Forest Service, Region 5, San Francisco, CA; Forest Service, Region 6, Portland, OR; Forest Service, Region 8, Atlanta, GA; Forest Service, Region 9, Milwaukee, WI; Forest Service, San Dimas, CA
USEUCOM (ECJ4/L-LO), Wright, Stuttgart, GE
USNA PWD Suprt. Annapolis MD
CANADA Defence & Civil Institute of Environ. Med, Downsview, Ontari
FLORIDA ATLANTIC UNIVERSITY Boca Raton FL (Ocean Engr Dept., C. Lin)
IOWA STATE UNIVERSITY Ames IA (CE Dept, Handy)
LEHIGH UNIVERSITY Bethlehem PA (Fritz Engr. Lab No. 13, Beedle); Bethlehem PA (Linder. an Lib. No.30, Fleckstein er)
LIBRAWY OF CONGRESS WASHINGTON, DC (SCIENCES & TECH DIV)
MICHIGAN TECHNOLOGICAL UNIVERSITY Houghton, MI (Haas)
MIT Cambridge MA; Cambridge MA (Rm 10-500, Tech. Reports, Engr. Lib.); NROTC (Collins) Cambridge MA
OREGON STATE UNIVERSITY CORVALLIS, OR (CE DEPT, BELL); CORVALLIS, OR (CE DEPT, HICKS)
PURDUE UNIVERSITY Lafayette IN (Leonards); Lafayette, IN (Altschaeffl); Lafayette, IN (CE Engr. Lib)
TEXAS A&M UNIVERSITY W.B. Ledbetter College Station, TX
UNIV OF MISSOURI - ROLLA Dept Mil Sci, Rolla, MD
UNIVERSITY OF CALIFORNIA BERKELEY, CA (CE DEPT, MITCHELL)
UNIVERSITY OF ILLINOIS Metz Ref Rm, Urbana IL; URBANA, IL (LIBRARY)
UNIVERSITY OF MASSACHUSETTS (Heronemus), Amherst MA CE Dept
UNIVERSITY OF NEBRASKA-LINCOLN Lincoln, NE (Ross Ice Shelf Proj.)
UNIVERSITY OF NEW MEXICO J Nielson-Engr Matls & Civil Sys Div, Albuquerque NM
UNIVERSITY OF WASHINGTON Seattle, WA Transportation, Construction & Geom. Div
AMETEK Offshore Res. & Engr Div
ARVID GRANT OLYMPI , WA
ATLANTIC RICHFIELD CO. DALLAS, TX (SMITH)
AUSTRALIA LNO, Army Mobile Equip R & D Com, Fort Belvoir VA; LNO. Fort Belvoir, VA
BECHTEL CORP. SAN FRANCISCO, CA (PHELPS)
BROWN & CALDWELL E M Saunders Walnut Creek, CA
CANADA Mem Univ Newfoundland (Chari), St Johns; Surveyor, Nenninger & Chenevert Inc., Montreal; Trans-Mnt Oil Pipe Lone Corp. Vancouver, BC Canada; W. German, Montreal, Quebec
DRAVO OCEAN STRUCTURES, INC. Metaire LA (J. Manson)
EBELLE M. SMITH ASSOC. INC Detriot MI (R. Ramos)
GLIDDEN CO. STRONGSVILLE, OH (RSCH LIB)
GULF COAST RSCH LAB. OCEAN SPRINGS, MS (LIBRARY)
HALEY & ALDRICH, INC. Cambridge MA (Aldrich, Jr.)
MC CLELLAND ENGINEERS INC Houston TX (B. McClelland)
MCDONNEL AIRCRAFT CO. Dept 501 (R.H. Fayman), St Louis MO

NORWAY J. Creed, Ski
PORTLAND CEMENT ASSOC. SKOKIE, IL (CORLEY; Skokie IL (Rsch & 8 ev Lab, Lib.)
R & D ASSOCIATES Marina Del Rey CA (H. Brode)
RAYMOND INTERNATIONAL INC. E Colle Soil Tech Dept, Pennsauken, NJ
SUN CONTROL SPECIALISTS (Duckwitz) Beltsville, MD
3 M Technical Library, St. Paul, MN
TIDEWATER CONSTR. CO Norfolk VA (Fowler)
UNITED KINGDOM Cement & Concrete Assoc Wexham Springs, Slough Bucks; Cement Marketing Co. Ltd. (Brittain) London; D. Lee, London; D. New, G. Maunsell & Partners, London; LNO, Army Mobile Equip R&D Com, Fort Belvoir VA
BULLOCK La Canada
ERVIN, DOUG Belmont, CA
R.F. BESIER Old Saybrook CT
WRIGLEY Salem MA